Identifying key plant traits and ecosystem properties affecting wave attenuation and the soil organic carbon content in tidal marshes

Identifying key plant traits and ecosystem properties affecting wave attenuation and the soil organic carbon content in tidal marshes

Schulte Ostermann, Tilla[1]; Heuner, Maike[2]; Fuchs, Elmar[2]; Temmerman, Stijn[3]; Schoutens, Ken[3]; Bouma, Tjeerd J.[4]; Minden, Vanessa[5]

[1]Landscape Ecology Group, University of Oldenburg, Oldenburg, Germany

[2]Department of Vegetation Studies and Landscape Management, Federal Institute of Hydrology, Koblenz, Germany

[3]Ecosphere Research Group, Department of Biology, University of Antwerp, Wilrijk, Belgium

[4]Royal Netherlands Institute of Sea Research, Yerseke, The Netherlands

[5]Department of Biology, Ecology and Biodiversity, Vrije Universiteit Brussel, Brussels, Belgium

Corresponding author: Vanessa Minden, Department of Biology, Ecology and Biodiversity, Vrije Universiteit Brussel, Brussels, Belgium. +32 2 629 3423, email: vanessa.minden@vub.be

Submission date: 24.05.2022

Abstract

Understanding the relationships among the environment, species traits and ecosystem properties is important for developing management measures that optimize the delivery of ecosystem services (ESs). Here, we identify the most important relationships responsible for the delivery of two key ESs provided by tidal marshes: (1) nature-based shoreline protection through wave attenuation and (2) mitigation of climate change through soil carbon storage. In two tidal zones below and above the mean high water (MHW, Elbe Estuary, Germany) level, we measured environmental parameters, such as soil salinity and inundation, as well as plant traits representing adaptations to hydrodynamic stress and strongly influencing decomposition rates.

Multiple linear regression results showed that wave attenuation rates were positively related to aboveground community biomass and stem bending resistance, and soil organic carbon was positively related to stem specific density (below the MHW level). In the tidal zone above the MHW level, soil carbon density was governed by inundation duration and decomposition rates.

Our study highlights that (1) ES delivery is not equally spread across tidal marshes and (2) ecosystem management should stimulate the development and persistence of habitat diversity (here, low and high marsh zones) to maximize ES delivery potential. Securing the delivery of the two studied ESs under climate change will depend on providing suitable (landward) space to sustain the functioning of the two marsh zones. In the studied marshes, these services are highly dependent on a few species (i.e., wave attenuation on *Schoenoplectus tabernaemontani* and *Bolboschoenus maritimus* and carbon storage on *Phragmites australis*), and as such, current and future ESs strongly depend on specific species' responses to changing environmental conditions.

Keywords: ecosystem properties, ecosystem services, estuarine vegetation, plant traits, soil organic carbon

Acknowledgements

We would like to thank Michael Kleyer for advice and support, Hannes Sahl and Thomas Jansen for measuring the elevations and Daniela Meißner in the laboratory, Frances Pusch for working on the initial phase of the project as well as the numerous students helping with sampling and processing work. This research was conducted in cooperation with the German Federal Institute of Hydrology (BfG) in line with its R&D-Project TIBASS (Tidal Bank Science and Services).

Introduction

Tidal estuaries are hotspots of valuable ecosystems, such as tidal marshes (Eertman et al. 2002; Waltham et al. 2021), as well as centres of human activities, such as ports, cities, and agricultural areas (Mitsch and Gosselink 2000). In the past, human land use development has often resulted in the loss of tidal marsh ecosystems (Bostrom et al. 2011), whereas currently there is an increasing demand for conservation and restoration of tidal marsh ecosystems (Gilby et al. 2021; Waltham et al. 2021). In many estuaries, human land use development is enabled by the construction of embankments and dikes to prevent flooding of human infrastructure (Aerts et al. 2014). Maintenance of artificial embankments is labour and cost intensive and with the issue of sea level rise, additional efforts, such as raising dikes, will demand for further investments (Vousdoukas et al. 2020; Klerk et al. 2021).

As such, and where possible, vegetation-based protection of estuarine shorelines is favoured over artificial embankments since natural vegetation attenuates waves (Barbier et al. 2011; Gedan et al. 2011), acts as a sediment trap (Coops et al. 1996), reduces flow velocities (Leonard and Luther 1995) and is potentially able to keep pace with rising sea levels (Kirwan

and Megonigal 2013; Temmerman and Kirwan 2015). The wave- and flow-reducing effect of plants has been the focus of many studies, for example, those on submerged plants (Bouma et al. 2005; Reidenbach and Thomas 2018), salt marsh plants (Leonard and Luther 1995; Bouma et al. 2010), brackish marshes (Schoutens et al. 2020) and mangroves (Horstman et al. 2014). In particular, short-period wind and swell waves can be strongly reduced through the friction and drag of coastal vegetation (Möller et al. 2014; Vuik et al. 2018). For example, Möller et al. (1999) showed that wave energy reduction was almost three times higher over a salt marsh than over a sand flat (82% versus 28.5%, respectively), and for mangroves, McIvor et al. (2012) reported a reduction in wave height of between 13% and 66% over 100 m of mangroves. Furthermore, despite their relatively small global extent, tidal marshes are important carbon sinks (Chmura et al. 2003; Ouyang and Lee 2020; Wang et al. 2021). Najjar et al. (2018) calculated the carbon budget for coastal waters of eastern North America and estimated that 20% of the entering carbon was buried and thus remained in the ecosystem. Similarly, McLeod et al. (2011) stressed that compared to terrestrial ecosystems, vegetated coastal ecosystems (such as mangrove forests and salt marshes) are important for their potential to sequester carbon dioxide.

In terms of coastal protection and climate change mitigation, the attenuation of waves and carbon storage are relevant ecosystem services (ESs) provided by tidal marshes. An ES is defined as an ecosystem property that benefits human welfare (Hooper et al. 2005; Millennium Ecosystem Assessment 2005). For example, the provision of firewood is a vegetation-based ES (Riis et al. 2020), that depends on biomass production, which in turn is an ecosystem property (Lavorel and Grigulis 2012). Ecosystem properties are the result of the interplay between specific plant traits and environmental factors; that is, plant traits vary in *response* to environmental conditions, while the resulting plant traits have an *effect* on ecosystem properties (Díaz et al. 2006; Díaz et al. 2007). This '*response-effect* framework' (Suding et al. 2008) has been tested on the ecosystem property of soil organic carbon content

in tidal marshes of the Elbe Estuary (Schulte Ostermann et al. 2021b). Across the whole elevation gradient from shore to the high bank, the authors showed that community biomass negatively responded to wave height and positively affected soil organic carbon content. This study showed that across the whole marsh, wave height was a key environmental factor strongly affecting plant traits. However, it remains unclear which plant traits had an effect on the rate of wave energy attenuation and soil organic carbon content in distinct parts of the marsh, namely, below and above the mean high water (MHW) level, respectively.

Tidal marshes are characterized by strong environmental gradients, such as inundation regimes, currents, wave energy and fluctuating soil salinity levels (Broome et al. 2019). All of these variables affect the tidal marsh vegetation at a descending magnitude from the low-elevation tidal flat up to the high-elevation river bank. The salinity levels of the river water create an additional descending gradient from the mouth of the river upstream (Cloern et al. 2017). In coastal marshes, tidal range in relation to the slope and elevation of the shore determines the frequency and duration of tidal inundation and has often been related to clear demarcations between vegetation zones (Eleuterius and Eleuterius 1979; Bockelmann et al. 2002). Generally, distinct vegetation can be found in a zone below mean high water (below MHW) and a zone above the mean high water (above MHW) level (Rayner et al. 2021; Schulte Ostermann et al. 2021a). The zone below the MHW level is inundated very regularly with saline water. Plants in this zone either have flexible stems to cope with drag forces (where wave energy is high) or have lignified, robust stems to withstand them (where wave energy is lower, Heuner et al. 2015). Furthermore, they are exposed to long periods of tidal inundation and potentially oxygen scarcity around their roots (Caudle and Maricle 2012; Carus et al. 2017). The upper zone, above the MHW level, is irregularly inundated, mainly during springtides or storm surges. In this zone, competition for light is a key interspecific driver (Coops et al. 1996; Craine and Dybzinski 2013; Carus et al. 2017). We expect that the abovementioned ES of soil organic carbon content is provided by the two zones below and

129 above the MHW level to different degrees, and wave energy attenuation is also provided by
130 the zone below the MHW level. Wave energy attenuation is expected to be one of the major
131 ESs of a lower marsh (below the MHW level), which is also exposed to higher wave stress
132 than the zone above the MHW level. For example, Schoutens et al. (2019) found wave height
133 reductions of up to 50% in *Bolboschoenus maritimus* L.-dominated vegetation below the
134 MHW level. In contrast, we expect soil organic carbon (SOC) content to be higher in a higher
135 marsh (above the MHW level), which is characterized by an extensive production of biomass
136 (Najjar et al. 2018). This biomass production, particularly belowground, has a strong impact
137 on the input of soil organic carbon (Rasse et al. 2005). Soil organic carbon is further related to
138 the species' traits, which affect the decomposition of biomass (Wardle et al. 2002) and
139 sedimentation dynamics; i.e., carbon is buried by mineral and organic sedimentation and
140 hence stored at increasing depths (Chmura et al. 2003; Mudd et al. 2009).
141 The objective of this study is to assess the impact of environmental variables, such as
142 inundation and soil salinity, on plant traits and to evaluate plant trait effects on the ESs (1)
143 wave attenuation and (2) soil carbon content in the zones below and above mean high water.
144 Thus, our study contributes to the development of effective ecosystem management measures,
145 with the aim of optimal provision of current and future ESs. For the zone below the MHW
146 level, we focused on both ESs, whereas in the zone above the MHW level, we only analysed
147 the effects on soil carbon content, as the incoming waves are already attenuated. We
148 measured different plant traits representing adaptations to hydrodynamic stress and strongly
149 influencing decomposition rates. For example, we expected wave attenuation to be affected
150 by plant traits that contribute to the structural support of plants or increase plant surface area,
151 such as high stem density and high leaf area, respectively (Puijalon et al. 2011; Schulte
152 Ostermann et al. 2021a). Plants with more flexible stems cope with wave energy, whereas
153 plants with stiffer stems withstand drag forces and are more resistant to mineralization
154 (Cornelissen and Thompson 1997; Heuner et al. 2015; Schoutens et al. 2020). We further

155 expected decomposition rates to be positively affected by a high leaf N:P ratio and negatively
156 affected by a high leaf dry matter content (White et al. 2004).
157
158 **Methods**
159 ***Study sites***
160 The Elbe River is one of the busiest and economically most important waterways of Germany
161 and Europe. Every year, sixty-six thousand ships navigate the tidal part of the Elbe River
162 connecting the Port of Hamburg with the North Sea, and of these ships, 90% are seagoing
163 vessels with an increasing number of particularly large ships (Wasserstraßen- und
164 Schifffahrtsdirektion Nord 2011; World Ports Sustainability Program 2018). These ships
165 create frequent waves (Hofmann et al. 2008), which add to the naturally created wind waves
166 and enhance the strain on both naturally vegetated tidal banks and artificially constructed dike
167 reinforcements (Silinski et al. 2015). To allow river access for more large ships, the riverbed
168 was deepened. This led to less bottom friction, faster landward tidal wave propagation and a
169 higher tidal range (Boehlich 2003) due to increased mean high water and decreased mean low
170 water levels (Butzeck et al. 2016). This dynamic caused increased sediment transport into the
171 system, as the tidal inflow is faster than the outgoing tidal ebb (Kerner 2007).
172 In the Elbe Estuary, three sites were chosen as study sites: Balje (53°51'30" N,
173 9°4'30"E), Hollerwettern (53°50'00"N, 9°22'30"E) and Krautsand (53°46'30"N, 9°22'0"E), see
174 Figure 1. For more information on the research areas, see Schoutens et al. (2019) and Schulte
175 Ostermann et al. (2021a). All sites have a gradually sloping topography with a landward
176 increase in soil surface elevation and a straight marsh edge. The climate at the sites is oceanic,
177 and the average temperature is 9.6 °C with annual precipitation of 831 mm (Cuxhaven,
178 Deutscher Wetterdienst 2021). The soils are sandy-silty, and agricultural activity is nearby but
179 not directly at the sites. Elevation was normalized relative to the tidal range, by which the
180 mean low water (MLW) level was set to 0 and the mean high water (MHW) level was set to

1. We did this to compare the elevations of the marsh edge and plant zones of sites with varying tidal ranges, following the equation $Znorm = \frac{Plot\ elevation - Mean\ Low\ Water}{(Mean\ High\ Water - Mean\ Low\ Water)}$ (see also Heuner et al. 2019). The mean tidal range is between 2.81 and 2.84 m, and the soil salinity ranges between 0.2 and 4 PSU (own measurements).

Sampling design

The sampling period was March 2016 to September 2017. By random stratified sampling, a total of 84 non-contiguous plots (4 m x 4 m) were distributed across the three sites, with 24 plots per site with a minimum distance of 20 m. The strata were elevation relative to tidal range and measured in each plot with real-time kinematic GPS, and vegetation zonation. For the vegetation zonation, we first defined tidal zones below mean the MHW level and above the MHW level with 42 plots in each zone, and within each of these tidal zones, we defined two distinct vegetation zones, with 21 plots in each zone. The first vegetation zone, closest to the marsh edge, contains monodominant stands of the leafless and flexible species *Schoenoplectus tabernaemontani* (C.C.Gmel.) and can be found up to 2 m under mean high water (Kötter 1961; Heuner et al. 2019). This vegetation is followed in landward direction by stands of *Bolboschoenus maritimus* (L.), a stiffer and taller sedge, still below the MHW level. At the mean high water level, *Phragmites australis* (Cav.) can establish and dominate in dense stands, distant from wave action because of its sensitivity towards mechanical stress (Coops et al. 1994; Ellenberg and Leuschner 2010). At 1 m above the MHW level, the fourth vegetation zone consists of a mixture of *P. australis* and other species, such as *Mentha aquatica* (L.) and *Juncus gerardii* (Loisel.) (Fig. 2).

Abiotic parameters

205 Inundation was determined by installing 80 cm long drainage pipes (8 cm diameter) in two
206 plots per vegetation zone and site, i.e., 24 pipes in total. The pipes were placed vertically in
207 the ground and equipped with pressure loggers (Sensus Ultra by Reefnet). The loggers
208 recorded hydrostatic and/or atmospheric pressure every hour between March and October
209 2016. Three additional loggers were positioned at each site on nearby buildings, to record the
210 corresponding air pressure (Minden and Kleyer 2014). Inundation was calculated from the
211 elevation of all plots (measured with real-time kinematic GPS) relative to the water level
212 recorded by the data loggers. The inundation period was set as the time during which the
213 water level was at ground level or above and expressed as hours per day.
214 Soil salinity of the topsoil was determined following Schlichting et al. (1995) by
215 diluting 10 g fresh soil with 25 ml H_2O and measuring conductivity in the excess water
216 (WTW ph/Cond340i/SET, Tetracon 325 electrode). Salinity was then calculated with the
217 UNESCO equation (UNESCO 1981; Grasshoff et al. 1983). In every plot, the soil was
218 sampled to a depth of 60 cm, and distinct soil horizons were identified if applicable. Wet and
219 dry bulk densities (g/cm³) were determined for 200 cm^3 for each detectable soil horizon by
220 weighing each sample fresh and dried, respectively (48 hours of drying at 105 °C, Schlichting
221 et al. 1995). The calcium carbonate ($CaCO_3$) content (kg/m) was measured following
222 Scheibler´s gasometric method (Schlichting et al. 1995). Grain size distribution (%, clay, silt
223 and sand content) was determined with a laser particle sizer (Analysette 22) after pre-
224 treatment with H_2O_2 to remove organic substances. Then, the value was related to the
225 determined bulk density and expressed as kg/m² for the profile depth of 80 cm.
226 Ammonium (NH_4) and nitrate (NO_3) contents were determined using the incubation
227 method following Gerlach (1973). The measurements were performed with a continuous flow
228 analyser (CFA) at 660 nm (ammonium) and 540 nm (nitrate) and then converted to mineral
229 nitrogen (N_{min}, g/m²). Soil phosphorus (P) and potassium (K) contents (g/m²) were determined
230 following the method of Egnér et al. (1960) and measured via a continuous flow analyser

231 (CFA, for phosphorus) or atomic adsorption spectroscopy (AAS, for potassium). Soil carbon
232 (C) content (g/m^2) was analysed with a C:N-Analyser (Flash 2000, Thermo Scientific)
233 following Allen (1989). Soil variables were extrapolated to a depth of 80 cm to be comparable
234 with those in other studies by multiplying the nutrient content (mass percentage) by the bulk
235 density and soil depth (Minden and Kleyer 2011; Minden and Kleyer 2015; Cebrián-Piqueras
236 2017). For details on all measured parameters, see Table 1, and for abiotic parameters below
237 and above the MHW level, see Fig. 3.
238
239 ***Frequency analysis of plant species and trait measurements***
240 Vegetation composition was recorded with a frequency frame (50 x 50 cm), which contained
241 25 cells, 10 x 10 cm each. The frame was used in all plots within a few consecutive days in
242 August 2016 four times per plot to cover a total area of 1 m² (Tremp 2005; Minden et al.
243 2012). In each cell, the presence or absence of a species was recorded. Species identity was
244 determined by the literature (Schmeil and Fitschen 2003; Rothmaler 2007). From all recorded
245 species, 17 species representing 95% of the total frequency were selected, and from these
246 species plant trait information was collected (Cornelissen et al. 2003). Information on species
247 names and their position below or above the MHW level is provided in Fig. 2.
248 A total of 175 plant individuals (at least 10 individuals per species) were collected at
249 the peak of their development, i.e., when seeds were ripe but not yet shed (Minden et al.
250 2012). To prevent damage to roots, a soil volume of approximately 20 x 20 x 40 cm was
251 excavated around the stem of each plant individual. Roots and rhizomes were cleaned with
252 water and separated from those of other plant individuals. Seeds, stems, leaves, roots and
253 rhizomes were sorted, dried for 72 hours at 70 °C and weighed. For the grass species, the leaf
254 area was measured as the leaf blades, and the petioles were assigned to the stem (following
255 Yan et al. 2016). For *S. tabernaemontani*, a leafless species, the green stem was used as an
256 equivalent to the leaf; only the belowground part that did not produce chlorophyll was treated

257 as the stem. The petioles of the species were excluded from specific leaf area (SLA)
258 measurements (Pérez-Harguindeguy et al. 2013).
259 Canopy height (cm) was determined in the field prior to harvesting (Weiher et al.
260 1999). For specific leaf area (SLA, (mm^2/mg)) two leaves per individual plant were cut off,
261 and their area (mm^2) was determined with a flatbed scanner (300dpi) and ImageJ software
262 (Rasband 1997-2018). The stem bending properties of the fresh samples were tested for at
263 least 20 stem segments per species across the three sites. Samples were stored under cool and
264 moist conditions with testing completed within a few days after harvest at the Royal
265 Netherlands Institute for Sea Research (NIOZ Yerseke, NL) with the Instron 5942 (Canton,
266 MA, USA, Heuner et al. 2015; Rupprecht et al. 2015). Young's modulus (MPa) describes the
267 resistance of a stem to bending and is a material characteristic (with higher values indicating
268 stiffer stems) derived from the slope of its stress-strain curve (Hamann and Puijalon 2013).
269 The equation used to calculate Young's modulus can be found in Appendix S1 (Coops and
270 Van der Velde 1996; Vuik et al. 2018).
271 For the mass per volume ($g_{fresh\ mass}/cm^3$) and specific density ($g_{dry\ mass}/cm^3$) of the
272 stems, roots, and rhizomes, volumetric flasks were used. Samples of the roots and rhizomes
273 (~2 cm per organ sample) of each collected plant individual were weighed in their fresh state,
274 their length was measured, and all material was finally dried and weighed (72 hours at 70 °C).
275 Specific root and rhizome length ($mm/g_{dry\ mass}$) and the dry matter content of each organ
276 ($mg_{dry\ mass}/g_{fresh\ mass}$) were determined. For each plant individual and organ, the carbon (C),
277 nitrogen (N) and phosphorus (P) contents (g/kg) were analysed. The C and N contents were
278 determined by grinding the material ('pulverizette 7', Fritsch, Idar-Oberstein, Germany) with
279 subsequent use of a C:N-analyzer (Flash 2000, Thermo Scientific) following Allen (1989). P
280 was extracted from the pulverized material (7-8 mg, precision balance, CP 225 D, Sartorius,
281 Goettingen, Germany) by heating the sample with nitric acid (95 °C, 6 hours) and then adding

hydrogen peroxide (30%, 95 °C, 4 hours). The volume was then raised to 1 ml with water (bidest) and measured via a CFA, following Murphy and Riley (1962).

Ecosystem properties

The aboveground biomass (AGB) was cut in August 2016 (De Leeuw et al. 1990). The vegetation was cut on 0.5 m² at ground level, subsequently dried (70 °C, 72 hours), weighed and extrapolated to 1 m² (Scurlock et al. 2002). Photosynthetically active radiation (PAR) reaching the soil surface was measured with a SunScan (Canopy Analysis System SS1, see Maier et al. 2010). This value was used as a measure of the vegetation density, with low measured values indicating denser vegetation. Approximately five measurements were taken in each plot, 5 cm above ground, and one additional measurement above the vegetation in full light was obtained. PAR was expressed as the percentage of the total radiation (%).

The decomposition rate at the plot level was determined by preparing mesh bags for each plot (1 mm wide meshes, Cebrián-Piqueras et al. 2017). Each bag was filled with 4 g of biomass from the same plot, and the exact weight was noted. To compare the decomposition rate across the sites, three bags per plot were filled with 'standard litter', i.e., hay. The bags were placed on top of the soil in each plot with the vegetation removed and were fixed with mesh. They were collected after 10 months, cleaned, dried and weighed (70 °C, 70 hours). The decomposition rate was expressed as % decomposed material per day (Minden and Kleyer 2015).

Ecosystem services

Wave heights were recorded at each site in one transect between December 2015 and April 2017 (Schoutens et al. 2019). At each of the three sites, three pressure sensors (P-Log3021-MMC, Driesen & Kern) were positioned along a cross-shore transect, with the first position on the unvegetated mudflat just in front of the vegetated marsh edge (i.e., measuring the

incoming waves not attenuated yet by vegetation), the second position 10 metres more landward from the marsh edge (i.e., measuring the waves that propagated through the *S. tabernaemontani* vegetation zone from position 1 to position 2), and the third position 20 metres from the marsh edge (i.e., measuring the waves that propagated through the *B. maritimus* zone from position 2 to 3). By correcting atmospheric pressure, the measurements (frequency of 8 Hz) were referenced to water surface elevation. The tidal signal was separated from the wave signal, but wind- or ship-generated waves were not distinguishable. A detailed description of the recording method can be found in Schoutens et al. (2019). In our study, we extrapolated wave attenuation for all plots for conditions when the water depth was less than 0.5 m and when the water depth varied over time (due to the tides) and between the plot locations (due to differences in plot surface elevations). For details on this process, see Appendix S2. The wave attenuation rate (m/m) was calculated as the vertical difference in wave height (in m) per horizontal distance (m) travelled by the waves between two measurement points, i.e., between positions 1 and 2 for wave attenuation in the *S. tabernaemontani* zone and positions 2 and 3 for wave attenuation in the *B. maritimus* zone (Schoutens et al. 2020). Hence, this rate was measured only for these two vegetation zones below the MHW level and not for the zones above the MHW level, as waves were already strongly attenuated by the time they reached the high and more landward positioned marsh zones (wave recordings were few in the *Phragmites* zone, Schoutens et al. 2020).

The soil organic carbon content (C, %) was determined with a C:N analyser (Flash 2000, Thermo Scientific, Allen 1989). The SOC content is the difference between the soil $CaCO_3$ content and the total carbon content (Cebrián-Piqueras et al. 2017). The soil organic carbon density (SOC density) (kg/m^3) was calculated from the SOC content (mass %) and the dry bulk density (kg/m^3) for the soil profile depth of 80 cm per plot and extrapolated to 1 m depths. For details on all measured parameters, see Table 1, and for ecosystem properties and services below and above the MHW level, see Fig. 2.

334

335 ***Statistical analysis***

336 To test whether the environmental and ecosystem property variables differed between the two
337 tidal zones below and above the MHW level, we used linear mixed effects models for each
338 variable. The two tidal zones (two levels, below the MHW level and above the MHW level)
339 were treated as explanatory variables, and the three study sites (three levels, Balje,
340 Hollerwettern and Krautsand) were treated as random effects
341 (lmer(environment~zone+(1|site)), R-package 'lme4', Bates et al. 2015). A pairwise test was
342 performed between the four vegetation zones (least squares means) for each model (R-
343 package 'emmeans', Lenth 2020). The degrees of freedom were based on the Kenward-Roger
344 method, and the p-value was adjusted with 'mvt' (Halekoh and Hojsgaard 2014). The
345 statistical analysis was conducted with the open source software R (R Core Team 2017) and
346 RStudio (RStudio Team 2021).

347 As a first step in analysing the effects of plant traits on the ESs, and as some plant
348 traits were strongly correlated, the plant traits were aggregated by a principal component
349 analysis (PCA). The scores of the first PCA axis were then used in the remaining analyses.
350 For this, the dataset was split into plots below the MHW level and above the MHW level, and
351 for each plot, the community weighted mean for each trait was calculated with the frequency
352 values of the specific plant species for this plot (community weighted means (CWM), Violle
353 et al. 2007; Cebrián-Piqueras et al. 2017). CWM-trait variables were then transformed to
354 conform to a normal distribution, where applicable (R-package 'stats', Royston 1982); see
355 Table 1. PCA analyses were run for groups of highly correlated traits.

356 To explore the relationship between different trait variables, standard major axis
357 regressions (SMA, Warton et al. 2006) were performed. This type of analysis is appropriate
358 when similar measurement errors are associated with both the X and Y variables, and thus,
359 common linear regression is not advised (Cui et al. 2020). The SMA summarizes the

relationship between two variables by minimizing the error of both variables, rather than predicting Y from X, for which ordinary least squares (OLS) regression would be adequate (Niklas 2006). SMA was performed with the R-package 'smatr' (Warton et al. 2012).

Finally, to explore the relationships among the environmental variables, plant traits and ecosystem properties, multiple linear regression (MLR) analysis was conducted. To meet the model assumptions, some variables were transformed (see Table 1). To find the best predictor for the ecosystem properties and ecosystem services, a stepwise selection was used to choose the best performing model with the lowest Akaike information criterion (AIC, Venables and Ripley 2002). The wire graphs (Figs. 5 and 6) were constructed with the R-package 'lattice' (Sarkar 2008).

Results

Environmental conditions, ecosystem properties and ecosystem services below and above the mean high water level

The environmental parameters clay content, soil P and K did not vary between the zones below and above the MHW level (Fig. 3, for each zone n=42, $p > 0.05$). All other variables varied between plots below and above the MHW level (for each zone n=42): inundation duration, soil salinity, soil carbonate content and soil sand content were higher below the MHW level than above the MHW level ($p<0.0001$ (inundation), $p=0.04$ (soil salinity), $p<0.0001$ (soil carbonate) and $p=0.002$ (soil sand content)), while plant available nitrogen was significantly lower below the MHW level than above the MHW level ($p=0.02$).

For the ecosystem properties, AGB ($p<0.001$) and decomposition rate of standard litter (hay, $p<0.001$) were higher in the zone above the MHW level than below the MHW level (for each zone n=42). In contrast, the decomposition of native biomass showed no differences between the two zones ($p>0.05$). Vegetation in the tidal zone below the MHW level was less

385 dense than that above the MHW level ($p<0.001$, expressed as PAR reaching the ground, with
386 low values indicating dense vegetation, see Fig. 4).
387 The ES wave attenuation was only measured at sites below the MHW level and ranged
388 between 0.012 and 0.036 m. The SOC content (%) and SOC density (kg/m^3) were both higher
389 in the zone above the MHW level (for each zone, n=42, $p<0.001$ and 0.02).
390
391 ***Relationships of plant traits and trait aggregates***
392 Traits for stem and leaf variables, biomass investment and stoichiometric composition of
393 leaves were highly positively correlated (Table 2, n=42 for each zone below and above the
394 MHW level, all $p < 0.05$, the corresponding PCA graphs are shown in Fig. S1). Stem mass per
395 volume, Young's modulus, stem specific density (SSD) and stem dry matter content (SDMC)
396 were aggregated into the variable 'stem traits'. Similarly, the variable 'leaf traits' comprised
397 the traits leaf dry matter content (LDMC) and total leaf area. The total biomass of stems,
398 leaves, roots and rhizomes were combined as 'mass'. For 'belowground traits', we aggregated
399 root dry matter content, rhizome dry matter content, root specific density, and rhizome
400 specific density, with inverted values, root specific length and rhizome specific length.
401 Finally, the variable 'leaf stoichiometry' comprised leaf ratios of N:P and C:N (see Table 1
402 for an overview of the aggregates). The highest amount of explained variance on the first
403 PCA axis was found for aggregate leaf stoichiometry (91% below the MHW level and 82%
404 above the MHW level), and the lowest explained variance was given by the aggregate
405 belowground traits (53% below the MHW level and 61% above the MHW level). Canopy
406 height was the only variable that was not aggregated via PCA, as it did not correlate strongly
407 with other variables (for correlation coefficients of traits with the first two PCA axes within
408 each trait aggregate see Table S1).

SMA regressions for trait aggregates below and above the MHW level yielded strong relationships for most of the trait combinations tested (Table 3, n=42 for each zone below and above MHW). Aggregates of the zone below the MHW level scaled both positively and negatively, whereas those of the zone above the MHW level only scaled positively (with the exception of canopy height versus stem traits, see slopes in Table 3). For example, plants with high biomass production showed low leaf area and low LDMC values, as well as low leaf N:P ratios in the zone below the MHW level (aggregates mass and leaf traits, slope -0.76, $p<0.01$, and mass and leaf stoichiometry, slope -1.17, $p<0.05$). Furthermore, a higher canopy was positively related to denser and stiffer support structures in both tidal zones (slope 0.14 below the MHW level and -0.15 above the MHW level, both $p<0.001$). The nutrient ratios within the leaves were positively related to the leaf trait aggregate: higher N:P ratios and lower C:N ratios were associated with a larger leaf area and higher dry matter content, irrespective of position along the elevation gradient. Similarly, the SMA results of stem traits versus leaf traits for both tidal zones highlighted the strong relationship between the underlying traits: higher SSD and Young's modulus were positively related to a larger leaf area (positive slopes Table 3, see Fig. S2 a and b).

Relationships between environmental variables, community weighted means of plant traits and ecosystem properties

The trait aggregates 'mass', 'belowground traits' and 'leaf stoichiometry' were not related to the measured ecosystem properties AGB, decomposition rates, SOC content and SOC density (n=42 for each zone below and above the MHW level, $p > 0.05$). These results were consistent for both tidal zones below or above the MHW level.

In the tidal zone below the MHW level, wave attenuation showed a positive relationship with AGB (Fig. 5a, Table 4, n=42, $p < 0.001$), indicating higher wave attenuation with higher AGB. The range of reduction in wave height at the plot level was between 0.01

435 and 0.05 m. Furthermore, and in line with our initial expectation, wave attenuation increased
436 linearly with the aggregate stem traits, which indicated that waves were attenuated in
437 productive communities comprised of species with stiff and dense stems. AGB increased with
438 leaf traits and stem traits (Fig. 5b, $p<0.01$ and <0.001, respectively). These aggregates
439 comprised LDMC and total leaf area (leaf traits) as well as the ratio of stem mass to volume,
440 SSD, stem dry matter content and Young's modulus. Their positive relationship with AGB
441 indicated that plant communities exhibiting traits related to slow growth and resistance to
442 disturbance showed high standing biomass (i.e., high AGB). Low SOC was associated with
443 low 'stem trait' values (i.e., less dense material and lower Young's modulus) and related
444 negatively with inundation duration, which describes plant communities with low stem
445 density at regularly inundated sites (Fig. 5c). The highest amounts of SOC were predicted for
446 the combination of intermediate 'stem traits' (SSD, fresh mass per volume, Young's modulus
447 and dry matter content, Fig. 5c, $p<0.05$) and low inundation ($p<0.01$).

448 For the vegetation zone above the MHW dominated by *P. australis*, the decomposition
449 rate of native plant material was strongly negatively related to inundation duration (Figure 6a,
450 Table 5, $n=42$, $p < 0.001$). This scenario was the strongest effect for the tidal zone above the
451 MHW level created by the inundation duration: with longer inundation, the decomposition
452 rates of the native biomass were significantly lower (Figure 6a). Furthermore, the relationship
453 between decomposition rates, inundation duration and 'stem traits' showed that decomposition
454 was highest when sites were weakly inundated and plant communities consisted of species
455 with intermediate stem trait values (Fig. 6a, $p<0.01$). These intermediate values of stem traits
456 describe plant communities with an average position in the range of stem stiffness and stem
457 flexibility.

458 The analysis of SOC density (kg/m³) revealed a bathtub-shaped relationship with stem
459 traits (Fig. 6b): the SOC density was lowest where the vegetation showed intermediate values
460 for Young's modulus, dry matter content and SSD ($p<0.05$). The SOC density was almost

linearly positively correlated with the decomposition rate of native biomass ($p<0.05$), which indicated that a high decomposition rate of community biomass led to high soil carbon density at these sites.

Discussion

Understanding the relationships between species traits, ecosystem properties, and ESs is important for developing effective measures of ecosystem management that contribute to the optimal delivery of ESs. In this paper, we identified such relationships for two ESs that are considered highly valuable in tidal marsh ecosystems, i.e., (1) wave attenuation, which contributes to nature-based mitigation of shoreline erosion and flood risks (Coops et al. 1996; Möller et al. 2014; Schoutens et al. 2019), and (2) soil carbon storage, which contributes to nature-based mitigation of climate warming (IPCC 2007; Hansen et al. 2017; Najjar et al. 2018). Our study revealed that the ES wave attenuation was most strongly affected by AGB and leaf and stem traits (i.e., traits contributing to stiff and dense stem material, as well as to a large leaf-surface area, such as high stem mass per volume, high SSD, high Young's modulus, and high leaf area) of the plant communities at these sites. The highest SOC content in the tidal marsh zone below the MHW level was determined by intermediate values of certain stem traits, such as SSD, fresh mass per volume, Young's modulus and dry matter content, as well as by low inundation levels. Interestingly, the same pattern led to the lowest SOC density in the tidal zone above the MHW level. We detected strong differences in the delivery of ESs between the vegetation zones above and below the MHW level, which highlights that a) the delivery of ESs is not necessarily equally spread across one habitat type and b) ecosystem management should be optimized to maximize the ESs delivery potential of the different vegetation zones.

Ecosystem services in the low tidal marsh zone (below the MHW level)

In the lower tidal marsh zone (below the MHW level), plant species diversity is relatively low because the species in this zone are exposed to harsh environmental conditions such as soil oxygen scarcity, higher soil salinity and longer inundation time (Takahashi et al. 2014). Additionally, hydrodynamic stress, such as strong waves, influences species composition, which often contains various types of shoreline vegetation (Odum 1988; Weiher and Keddy 1999). For example, in an estuary in Rhode Island, USA, van Wesenbeeck et al. (2007) found distinct habitat types along a hydrodynamic gradient. Species' responses to these environmental conditions (e.g., small stature under strong wave exposure or reduced growth under salt stress, Ungar 1991; Coops et al. 1994) may affect the ES of wave attenuation.

In the tidal zone below the MHW level, we found positive correlations of higher Young's modulus (higher stem resistance to bending) with higher wave attenuation (Augustin et al. 2009; Möller et al. 2014; Schoutens et al. 2019). Within the trait aggregate stem traits, Young's modulus showed a positive relationship to SSD. This is an intriguing finding, as SSD is easier to determine, with less laboratory equipment needed, and therefore could offer a good alternative to stem bending properties, and SSD also takes the volume of the stem into account. Investment in stiffer stems also means a higher drag force resulting from waves will be experienced (Bouma et al. 2005); therefore, a greater risk of breakage or buckling of stems under the influence of wave energy will occur. The vegetation of the lower tidal marsh zone is characterized by a rough surface structure and enlarged surface area, which together create more friction with the incoming water, which then reduces the wave energy (see also Möller et al. 1999; Heuner et al. 2015). Our results support this, as they show an indirect effect of the leaf traits aggregate on wave attenuation through aboveground biomass. We found that the total leaf area and LDMC of the plant community were positively related to AGB and that higher AGB was correlated with higher wave attenuation rates. Similar results were found for *S. tabernaemontani* and *B. maritimus* in flume channel experiments (see also Heuner et al. 2015; Rupprecht et al. 2015). Schoutens et al. (2019) found that in the Elbe Estuary waves

513 (with a mean significant height of 0.09 m) were attenuated up to 50% over a 10 m transect of
514 vegetation. In other habitats, AGB was shown to be strongly positively influenced by soil
515 fertility and negatively influenced by incoming waves, inundation and salinity (Lillebo et al.
516 2003; Crain 2007; van Wesenbeeck et al. 2007; Minden and Kleyer 2015). The only
517 detectable difference in soil nutrient content in this study was found for N_{min}, with less
518 available nitrogen below the MHW level, but this was not correlated with AGB.
519 AGB was positively related to leaf traits and stem traits, indicating that in the zone
520 below the MHW level, a high AGB occurred when plants exhibited stiff stems and large leaf
521 areas. Similarly, a high leaf area and high Young's modulus were found to be positively
522 correlated with AGB when the whole gradient from tidal flat to upper marsh was taken into
523 account (Schulte Ostermann et al. 2021b). Other studies have shown that salinity levels
524 affected biomass production, with lower biomass production under high salinity levels, as
525 plants invest part of their resources into salt defence mechanisms rather than into growth
526 (succulent growth or excretion of salt from their tissues, Flowers and Colmer 2008). For
527 example, biomass production in salt marshes was determined at 467 g/m^2 (Minden 2010,
528 similar results were found by Rupprecht et al., 2015) compared to an average of 700-900 g/m^2
529 for brackish marshes at low elevations (Schoutens et al. 2019).
530 Finally, related to SOC content, succulent growth as a response to salinity has been
531 related to plant tissue decomposability, with succulent plants decomposing more rapidly
532 (Zedler et al. 1980). This scenario may have repercussions on carbon cycling and possibly the
533 carbon sink function of the ecosystem. The present analyses show that decomposition rates at
534 elevations below the MHW level in our study area were mainly governed by the inundation
535 regime, possibly through effects on the microbial community (Wang et al. 2019). In response
536 to inundation, plants produce less dense belowground organs with low dry matter content
537 (Schulte Ostermann et al. 2021a). This, combined with the effects of soil salinity on AGB and
538 ramet height (Carus et al. 2017), could explain the relatively low soil organic carbon

concentrations below the MHW level: the biomass produced was low and showed a low dry matter content with a high mineralization rate. The incoming waves also relocate biomass and wash it out of the system (Hansen et al. 2017, potentially also bring biomass and sediment into the system), but the mesh bags in our study were fixed on the ground, and the mesh size of 1 mm² prevented biomass from exiting the bags, so we considered these effects as nonsignificant.

Ecosystem services in the high tidal marsh zone (above the MHW level)

In the present study, the mean SOC density in the tidal zone above the MHW level was 15 kg/m³ compared to 10 kg/m³ in the zone below the MHW level, which is similar to the results of other studies. For example, Peck et al. (2020) measured the mean soil organic carbon density on average to be between 10 and 45 kg/m³ in estuaries in Oregon, USA, whereas a mean of 27 kg/m³ was calculated at over almost 2000 sites across the USA by Holmquist et al. (2018). In the vegetation zone above the MHW level, we found that SOC density was strongly influenced by the traits of the plant community, namely, the stem traits aggregate, and decomposition rates of plant biomass. The stem trait aggregate and SOC density showed a bathtub-shaped relationship: SOC density was highest at both ends of the bathtub, i.e., where the vegetation showed high and low values of Young's modulus, dry matter content and SSD. In contrast, SOC density was lowest at intermediate values of these measured plant traits. Furthermore, the higher SOC density in the plots above the MHW level was related to higher decomposition rates, which seems contradictory, as the decomposition process breaks down organic material (Robertson and Paul 2000). We could not find significant relationships between SOC density and either aboveground or belowground community biomass, which was expected, especially for belowground biomass, as it is essential for the potential to store carbon in soil (Rasse et al. 2005; Chmura 2013). The position below the soil surface protects the plant organs from most of the physical disturbance, and they are less likely to be flushed

565 away. Thus, allocation to belowground biomass strongly drives SOC in a plant community
566 (Jobbagy and Jackson 2000; Rasse et al. 2005). However, in our study, we could not establish
567 a relationship between the belowground trait aggregate and SOC density.
568 For SOC density, decomposition rates were also strongly influenced by the stem trait
569 aggregate, as well as by inundation rates. The hampering effects of inundation on
570 decomposition rates are in concordance with the findings of Janousek et al. (2017), who found
571 higher decomposition at marsh sites with low inundation levels. However, Kirwan et al.
572 (2013) found both no effect of flooding on decomposition and even higher decomposition
573 rates with higher inundation. For a subarctic flora, Cornelissen et al. (2004) found lignin/N
574 leaf concentrations to be correlated with decomposability, while Freschet et al. (2012) found
575 traits related to structure (lignin, dry matter content and C) to control decomposition (see also
576 Güsewell and Verhoeven 2006; Liu et al. 2017). Surprisingly, for our study, we could not
577 relate leaf stoichiometry to decomposition rates, possibly because the effect of inundation was
578 overriding that of leaf chemical properties.
579
580 ***Implications for the management of tidal marshes with a special focus on the Elbe Estuary***
581 In addition to the changes that climate change may induce to plant species zonation in
582 estuarine systems, the Elbe Estuary and its tidal marshes, where our study took place, are also
583 facing challenges due to the deepening of the riverbed, to allow access to larger ships and
584 reduced space for floodplains from embankment construction (HPA and WSA 2011). Natural
585 floodplains have already been reduced by 75% since 1902 (Kappenberg and Fanger 2007).
586 The deepening of the Elbe River in 1999 produced a decrease of 25% in the outflow velocities
587 during low tide, which in turn affected the landward, upstream sediment transport, which
588 increased by 20% in Hamburg Harbour and by 120% along the freshwater longitudinal profile
589 (Kerner 2007). An important threat to tidal marsh vegetation is sea level rise, which may
590 affect species zonation and may further reduce the size of the flood plain (Reise 2005; Zhu et

591 al. 2020). Many studies have shown that the elevation of a site relative to the MHW level can
592 be used as a key predictor for the distribution of a species (Bertness and Ellison 1987;
593 Bockelmann et al. 2002; Suchrow and Jensen 2010). Although studies have shown that
594 marshes can keep pace with sea level rise through vertical sediment accretion (Temmerman
595 and Kirwan 2015; Kirwan et al. 2016), the accretion rate may be insufficient, eventually
596 leading to marsh inundation if the sea level rises too quickly (Schepers et al. 2017;
597 Himmelstein et al. 2021). This scenario reduces their potential to attenuate waves and may
598 result in a greater necessary investment for artificial bank enforcements. As Temmerman and
599 Kirwan (2015) noted, nature-based solutions will be more sustainable, especially with rising
600 energy costs for artificial structures (see also Temmerman et al. 2013).
601 The plant traits analysed in the present study showed strong correlations with each
602 other, following the concept of allometric scaling, and this finding was similar in the tidal
603 marsh zones below and above the MHW level. For the two ESs wave attenuation and carbon
604 storage, we found that the effects of plant traits on these ESs differed between the tidal zones
605 below and above the MHW level. While wave attenuation was strongly influenced by stem
606 and leaf traits, carbon storage was dependent on stem traits, as well as on inundation duration.
607 For the ES wave attenuation, we found that in this study the AGB was essential. The
608 zonation of species at the study sites in the marsh zone below the MHW level contained
609 smaller and more flexible *S. tabernaemontani* at the lowest elevations closest to the river
610 channel, with *B. maritimus* at higher elevations, with more biomass and greater effect on
611 wave attenuation. For carbon density, the biomass production of *P. australis* at higher,
612 infrequent inundation sites was important, as this species produces dense fibres and makes up
613 most of the biomass present. One possibility for increasing the carbon density potential of the
614 area would be to allow the extension of the *P. australis* vegetation zone into the adjacent
615 agricultural grasslands. In our opinion, a key aspect of future management of the tidal marsh
616 should be allowing for sufficient space landward. This would sustain the functioning of the

lower and higher marsh vegetation zones; for example, the carbon storage potential of the higher marsh is dependent on the wave attenuation function of the lower marsh. In fact, allowing for more flooding space is a management strategy in salt marshes (Wolters et al. 2005). However, the success of these practices will also depend on the supply of sediment, land use practices upstream and the specific species' responses to climate change (Kirwan and Megonigal 2013).

Data availability

Data on plant traits are publicly available through the Dryad repository (https://doi.org/10.5061/dryad.qjq2bvqmv). Data on soil carbon content and density will be made available through the Coastal Carbon Research Coordination Network (smithsonian.github.io/CCN-Community-Resources) upon article publication.

Literature

Aerts, J., W.J.W. Botzen, K. Emanuel, N. Lin, H. de Moel, and E.O. Michel-Kerjan. 2014. Evaluating flood resilience strategies for coastal megacities. *Science* 344: 472-474.

Allen, S.E. 1989. *Chemical analysis of ecological materials*. Oxford, England: Blackwell Scientific Publications.

Augustin, L.N., J.L. Irish, and P. Lynett. 2009. Laboratory and numerical studies of wave damping by emergent and near-emergent wetland vegetation. *Coastal Engineering* 56: 332-340.

Barbier, E.B., S.D. Hacker, C. Kennedy, E.W. Koch, A.C. Stier, and B.R. Silliman. 2011. The value of estuarine and coastal ecosystem services. *Ecological Monographs* 81: 169-193.

Bates, D., M. Maechler, B. Bolker, and S. Walker. 2015. Fitting linear mixed-effects models using lme4. *Journal of Statistical Software* 67: 1-48.

Bertness, M.D., and A.M. Ellison. 1987. Determinants of pattern in a New England salt marsh plant community. *Ecological Monographs* 57: 129-147.

644 Bockelmann, A.C., J.P. Bakker, R. Neuhaus, and J. Lage. 2002. The relation between
645 vegetation zonation, elevation and inundation frequency in a Wadden Sea salt marsh.
646 *Aquatic Botany* 73: 211-221.
647 Boehlich, M.J. 2003. Tidedynamik der Elbe. *Mitteilungsblatt der Bundesanstalt für*
648 *Wasserbau* 86: 55-60.
649 Bostrom, C., S.J. Pittman, C. Simenstad, and R.T. Kneib. 2011. Seascape ecology of coastal
650 biogenic habitats: advances, gaps, and challenges. *Marine Ecology Progress Series* 427:
651 191-217.
652 Bouma, T.J., M.B. De Vries, and P.M.J. Herman. 2010. Comparing ecosystem engineering
653 efficiency of two plant species with contrasting growth strategies. *Ecology* 91: 2696-
654 2704.
655 Bouma, T.J., M.B. De Vries, E. Low, G. Peralta, I.C. Tánczos, J. van de Koppel, and P.M.J.
656 Herman. 2005. Trade-offs related to ecosystem engineering: a case study on stiffness of
657 emerging macrophytes. *Ecology* 86: 2187-2199.
658 Broome, S.W., C.B. Craft, and M.R. Burchell. 2019. Tidal Marsh Creation. In *Coastal*
659 *Wetlands: An Integrated Ecosystem Approach*, ed. G.M.E. Perillo, E. Wolanski, D.R.
660 Cahoon and C.S. Hopkinson, 789-816: Elsevier.
661 Butzeck, C., U. Schroder, J. Oldeland, S. Nolte, and K. Jensen. 2016. Vegetation succession
662 of low estuarine marshes is affected by distance to navigation channel and changes in
663 water level. *Journal of Coastal Conservation* 20: 221-236.
664 Carus, J., M. Heuner, M. Paul, and B. Schroder. 2017. Plant distribution and stand
665 characteristics in brackish marshes: Unravelling the roles of abiotic factors and
666 interspecific competition. *Estuarine Coastal and Shelf Science* 196: 237-247.
667 Caudle, K.L., and B.R. Maricle. 2012. Effects of flooding on photosynthesis, chlorophyll
668 fluorescence, and oxygen stress in plants of varying flooding tolerance. *Transactions of*
669 *the Kansas Academy of Science* 115: 5-18.
670 Cebrián-Piqueras, M.A. 2017. Trade-offs and synergies between forage production, species
671 conservation and carbon stocks in temperate coastal wet grasslands. An ecosystem
672 services and process-based approach, Dissertation. University of Oldenburg Oldenburg.
673 Cebrián-Piqueras, M.A., J. Trinogga, C. Grande, V. Minden, M. Maier, and M. Kleyer. 2017.
674 Interactions between ecosystem properties and land use clarify spatial strategies to
675 optimize trade-offs between agriculture and species conservation. *International Journal*
676 *of Biodiversity Science, Ecosystem Services and Management* 13: 53-66.

677 Chmura, G.L. 2013. What do we need to assess the sustainability of the tidal salt marsh
678 carbon sink? *Ocean & Coastal Management* 83: 25-31.
679 Chmura, G.L., S.C. Anisfeld, D.R. Cahoon, and J.C. Lynch. 2003. Global carbon
680 sequestration in tidal, saline wetland soils. *Global Biogeochemical Cycles* 17: 22.
681 https://doi.org/10.1029/2002GB001917.
682 Cloern, J.E., A.D. Jassby, T.S. Schraga, E. Nejad, and C. Martin. 2017. Ecosystem variability
683 along the estuarine salinity gradient: Examples from long-term study of San Francisco
684 Bay. *Limnology and Oceanography* 62: S272-S291.
685 Coops, H., N. Geilen, and G. Vandervelde. 1994. Distribution and growth of helophte species
686 *Phragmites australis* and *Scirpus lacustris* in water depth gradients in relation to wave
687 exposure. *Aquatic Botany* 48: 273-284.
688 Coops, H., N. Geilen, H.J. Verheij, R. Boeters, and G. vanderVelde. 1996. Interactions
689 between waves, bank erosion and emergent vegetation: An experimental study in a
690 wave tank. *Aquatic Botany* 53: 187-198.
691 Coops, H., and G. Van der Velde. 1996. Effects of waves on helophyte stands: Mechanical
692 characteristics of stems of *Phragmites australis* and *Scirpus lacustris*. *Aquatic Botany*
693 53: 175-185.
694 Cornelissen, J.H.C., S. Lavorel, E. Garnier, S. Diaz, N. Buchmann, D.E. Gurvich, P.B. Reich,
695 H. ter Steege, H.D. Morgan, M.G.A. van der Heijden, J.G. Pausas, and H. Poorter. 2003.
696 A handbook of protocols for standardised and easy measurement of plant functional
697 traits worldwide. *Australian Journal of Botany* 51: 335-380.
698 Cornelissen, J.H.C., H.M. Quested, D. Gwynn-Jones, R.S.P. Van Logtestijn, M.A.H. De
699 Beus, A. Kondratchuk, T.V. Callaghan, and R. Aerts. 2004. Leaf digestibility and litter
700 decomposability are related in a wide range of subarctic plant species and types.
701 *Functional Ecology* 18: 779-786.
702 Cornelissen, J.H.C., and K. Thompson. 1997. Functional leaf attributes predict litter
703 decomposition rates in herbaceous plants. *New Phytologist* 135: 109-114.
704 Crain, C.M. 2007. Shifting nutrient limitation and eutrophication effects in marsh vegetation
705 across estuarine salinity gradients. *Estuaries and Coasts* 30: 26-34.
706 Craine, J.M., and R. Dybzinski. 2013. Mechanisms of plant competition for nutrients, water
707 and light. *Functional Ecology* 27: 833-840.
708 Cui, E.Q., E.S. Weng, E.R. Yan, and J.Y. Xia. 2020. Robust leaf trait relationships across
709 species under global environmental changes. *Nature Communications* 11: 2999.
710 https://doi.org/10.1038/s41467-020-16839-9.

De Leeuw, J., H. Olff, and J.P. Bakker. 1990. Year-to-year variation in peak above-ground biomass of six salt-marsh angiosperm communities as related to rainfall deficit and inundation frequency. *Aquatic Botany* 36: 139-151.

Deutscher Wetterdienst. 2021. Mean Climate Values for the Period 1981 to 2010.

Díaz, S., J. Fargione, I.F.S. Chapin, and D. Tilman. 2006. Biodiversity loss threatens human well-being. *PLoS Biology* 4: 1300-1305.

Díaz, S., S. Lavorel, F. De Bello, F. Quétier, K. Grigulis, and M.T. Robson. 2007. Incorporating plant functional diversity effects in ecosystem service assessments. *Proceedings of the National Academy of Sciences* 104: 20684-20689.

Eertman, R.H.M., B.A. Kornman, E. Stikvoort, and H. Verbeek. 2002. Restoration of the Sieperda tidal marsh in the Scheldt estuary, the Netherlands. *Restoration Ecology* 10: 438-449.

Egnér, H., H. Riehm, and W.R. Domingo. 1960. Untersuchungen über die Bodenanalyse als Grundlage für die Beurteilung des Nährstoffzustandes des Bodens II. Chemische Extraktionsmethoden zur Phosphor- und Kaliumbestimmung. *Kungl. Lantbrukshögskolans Annualer* 26: 199-215.

Eleuterius, L.N., and C.K. Eleuterius. 1979. Tide levels and salt-marsh zonation. *Bulletin of Marine Science* 29: 394-400.

Ellenberg, H., and C. Leuschner. 2010. *Vegetation Mitteleuropas mit den Alpen*. Stuttgart: Eugen Ulmer Verlag.

Flowers, T.J., and T.D. Colmer. 2008. Salinity tolerance in halophytes. *New Phytologist* 179: 945-963.

Freschet, G.T., R. Aerts, and J.H.C. Cornelissen. 2012. A plant economics spectrum of litter decomposability. *Functional Ecology* 26: 56-65.

Gedan, K.B., M.L. Kirwan, E. Wolanski, E.B. Barbier, and B.R. Silliman. 2011. The present and future role of coastal wetland vegetation in protecting shorelines: answering recent challenges to the paradigm. *Climatic Change* 106: 7-29.

Gerlach, A. 1973. *Methodische Untersuchungen zur Bestimmung der Stickstoffmineralisation*. Göttingen: Verlag Erich Golze, KG.

Gilby, B., M.P. Weinstein, R. Baker, J. Cebrian, S.B. Alford, A. Chelsky, D. Colombano, R.M. Connolly, C.A. Currin, I.C. Feller, A. Frank, J.A. Goeke, L.G.A. Gaines, F.E. Hardcastle, C.J. Henderson, C.W. Martin, A.E. McDonald, B.H. Morrison, A.D. Olds, J.S. Rehage, N.J. Waltham, and S.L. Ziegler. 2021. Human actions alter tidal marsh seascapes and the provision of ecosystem services. *Estuaries and Coasts* 44: 1628-1636.

745 Grasshoff, K., M. Ehrhardt, and K. Kremling. 1983. *Methods of Seawater Analysis*.
746 Weinheim, Germany: Verlag Chemie: Wiley.
747 Güsewell, S., and J.T.A. Verhoeven. 2006. Litter N : P ratios indicate whether N or P limits
748 the decomposability of graminoid leaf litter. *Plant and Soil* 287: 131-143.
749 Halekoh, U., and S. Hojsgaard. 2014. Kenward-Roger approximation and parametric
750 bootstrap methods for tests in linear mixed models: the R package pbkrtest. *Journal of*
751 *Statistical Software* 59: 1-32.
752 Hamann, E., and S. Puijalon. 2013. Biomechanical responses of aquatic plants to aerial
753 conditions. *Annals of Botany* 112: 1869-1878.
754 Hansen, K., C. Butzeck, A. Eschenbach, A. Grongroft, K. Jensen, and E.M. Pfeiffer. 2017.
755 Factors influencing the organic carbon pools in tidal marsh soils of the Elbe estuary
756 (Germany). *Journal of Soils and Sediments* 17: 47-60.
757 Heuner, M., B. Schroder, U. Schroder, and B. Kleinschmit. 2019. Contrasting elevational
758 responses of regularly flooded marsh plants in navigable estuaries. *Ecohydrology &*
759 *Hydrobiology* 19: 38-53.
760 Heuner, M., A. Silinski, J. Schoelynck, T.J. Bouma, S. Puijalon, P. Troch, E. Fuchs, B.
761 Schröder, U. Schröder, P. Meire, and S. Temmerman. 2015. Ecosystem engineering by
762 plants on wave-exposed intertidal flats is governed by relationships between effect and
763 response traits. *PLOS One* 10: e0138086. https://doi.org/10.1371/journal.pone.0138086.
764 Himmelstein, J., O.D. Vinent, S. Temmerman, and M.L. Kirwan. 2021. Mechanisms of pond
765 expansion in a rapidly submerging marsh. *Frontiers in Marine Science* 8: 704768.
766 https://doi.org/10.3389/fmars.2021.704768.
767 Hofmann, H., A. Lorke, and F. Peeters. 2008. The relative importance of wind and ship waves
768 in the littoral zone of a large lake. *Limnology and Oceanography* 53: 368-380.
769 Holmquist, J.R., L. Windham-Myers, N. Bliss, S. Crooks, J.T. Morris, J.P. Megonigal, T.
770 Troxler, D. Weller, J. Callaway, J. Drexler, M.C. Ferner, M.E. Gonneea, K.D. Kroeger,
771 L. Schile-Beers, I. Woo, K. Buffington, J. Breithaupt, B.M. Boyd, L.N. Brown, N. Dix,
772 L. Hice, B.P. Horton, G.M. MacDonald, R.P. Moyer, W. Reay, T. Shaw, E. Smith, J.M.
773 Smoak, C. Sommeffield, K. Thorne, D. Velinske, E. Watson, K.W. Grimes, and M.
774 Woodrey. 2018. Accuracy and precision of tidal wetland soil carbon mapping in the
775 conterminous United States. *Scientific Reports* 8: 9478. https://doi.org/10.1038/s41598-
776 018-26948-7.
777 Hooper, D.U., F.S. Chapin III, J.J. Ewel, A. Hector, P. Inchausti, S. Lavorel, J.H. Lawton,
778 D.M. Lodge, M. Loreau, S. Naeem, B. Schmid, H. Setälä, A.J. Symstad, J. Vandermeer,

779 and W.D. A. 2005. Effects of biodiversity on ecosystem functioning: a consensus of
780 current knowledge and needs for further research. *Ecological Monographs* 75: 3-35.
781 Horstman, E.M., C.M. Dohmen-Janssen, P.M.F. Narra, N.J.F. van den Berg, M. Siemerink,
782 and S. Hulscher. 2014. Wave attenuation in mangroves: A quantitative approach to field
783 observations. *Coastal Engineering* 94: 47-62.
784 HPA, and WSA. 2011. Hamburg Port Authority and Federal Waterways and Shipping
785 Administration: River Elbe engineering and sediment management concept. Review of
786 sediment management strategy in the context of other European estuaries from a
787 morphological perspective. Report Nr. 1805.
788 IPCC. 2007. *Climate Change 2007: Synthesis Report. Contribution of Working Groups I, II*
789 *and III to the fourth assessment report of the intergovernmental panel on climate*
790 *change*. Geneva, Switzerland: IPCC.
791 Janousek, C.N., K.J. Buffington, G.R. Guntenspergen, K.M. Thorne, B.D. Dugger, and J.Y.
792 Takekawa. 2017. Inundation, vegetation, and sediment effects on litter decomposition in
793 pacific coast tidal marshes. *Ecosystems* 20: 1296-1310.
794 Jobbagy, E.G., and R.B. Jackson. 2000. The vertical distribution of soil organic carbon and its
795 relation to climate and vegetation. *Ecological Applications* 10: 423-436.
796 Kappenberg, J., and H.U. Fanger. 2007. *Sedimenttransportgeschehen in der tidebeeinflussten*
797 *Elbe, der Deutschen Bucht und in der Nordsee*. Geesthacht: GKSS-Forschungszentrum
798 Geesthacht GmbH.
799 Kerner, M. 2007. Effects of deepening the Elbe estuary on sediment regime and water quality.
800 *Estuarine Coastal and Shelf Science* 75: 492-500.
801 Kirwan, M.L., J.A. Langley, G.R. Guntenspergen, and J.P. Megonigal. 2013. The impact of
802 sea-level rise on organic matter decay rates in Chesapeake Bay brackish tidal marshes.
803 *Biogeosciences* 10: 1869-1876.
804 Kirwan, M.L., and J.P. Megonigal. 2013. Tidal wetland stability in the face of human impacts
805 and sea-level rise. *Nature* 504: 53-60.
806 Kirwan, M.L., S. Temmerman, E.E. Skeehan, G.R. Guntenspergen, and S. Fagherazzi. 2016.
807 Overestimation of marsh vulnerability to sea level rise. *Nature Climate Change* 6: 253-
808 260.
809 Klerk, W.J., W. Kanning, M. Kok, and R. Wolfert. 2021. Optimal planning of flood defence
810 system reinforcements using a greedy search algorithm. *Reliability Engineering &*
811 *System Safety* 207: 107344. https://doi.org/10.1016/j.ress.2020.107344.

812 Kötter, F. 1961. Die Pflanzengesellschaften im Tidegebiet der Unterelbe. *Archiv für*
813 *Hydrobiologie*: 106-184.
814 Lavorel, S., and K. Grigulis. 2012. How fundamental plant functional trait relationships scale-
815 up to trade-offs and synergies in ecosystem services. *Journal of Ecology* 100: 128-140.
816 Lenth, R. 2020. Emmeans: Estimated Marginal Means, Aka Least-squares Means. R Package
817 Version 1.5.0.
818 Leonard, L.A., and M.E. Luther. 1995. Flow hydrodynamics in tidal marsh canopies.
819 *Limnology and Oceanography* 40: 1474-1484.
820 Lillebo, A.I., M.A. Pardal, J.M. Neto, and J.C. Marques. 2003. Salinity as the major factor
821 affecting *Scirpus maritimus* annual dynamics: evidence from field data and greenhouse
822 experiment. *Aquatic Botany* 77: 111-120.
823 Liu, G.D., J.F. Sun, K. Tian, D.R. Xiao, and X.Z. Yuan. 2017. Long-term responses of leaf
824 litter decomposition to temperature, litter quality and litter mixing in plateau wetlands.
825 *Freshwater Biology* 62: 178-190.
826 Maier, M., J. Schwienheer, K.-M. Exo, and J. Stahl. 2010. Vegetation structure of TMAP
827 vegetation types on mainland salt marshes. *Wadden Sea Ecosystem* 26: 105-110.
828 McIvor, A.L., T. Spencer, I. Möller, and M. Spalding. 2012. Storm surge reduction by
829 mangroves. In *Natural Coastal Protection Series: Report 2*, 36. Cambridgem UK: The
830 NatureConservancy, University of Cambridge, and Wetlands International.
831 McLeod, E., G.L. Chmura, S. Bouillon, R. Salm, M. Bjork, C.M. Duarte, C.E. Lovelock,
832 W.H. Schlesinger, and B.R. Silliman. 2011. A blueprint for blue carbon: toward an
833 improved understanding of the role of vegetated coastal habitats in sequestering CO2.
834 *Frontiers in Ecology and the Environment* 9: 552-560.
835 Millennium Ecosystem Assessment. 2005. *Ecosystems and Human Well-being: Synthesis*.
836 Washington DC: Island Press.
837 Minden, V. 2010. Functional traits of salt marsh plants: responses of morphology- and
838 elemental- based traits to environmental constraints, trait-trait relationships and effects
839 on ecosystem properties, University of Oldenburg Oldenburg, Germany.
840 Minden, V., S. Andratschke, J. Spalke, H. Timmermann, and M. Kleyer. 2012. Plant trait-
841 environment relationships in salt marshes: Deviations from predictions by ecological
842 concepts. *Perspectives in Plant Ecology Evolution and Systematics* 14: 183-192.
843 Minden, V., and M. Kleyer. 2011. Testing the effect-response framework: key response and
844 effect traits determining aboveground biomass of salt marshes. *Journal of Vegetation*
845 *Science* 22: 387-401.

846 Minden, V., and M. Kleyer. 2014. Internal and external regulation of plant organ
847 stoichiometry. *Plant Biology* 16: 897-907.
848 Minden, V., and M. Kleyer. 2015. Ecosystem multifunctionality of coastal marshes is
849 determined by key plant traits. *Journal of Vegetation Science* 26: 651-662.
850 Mitsch, W.J., and J.G. Gosselink. 2000. The value of wetlands: importance of scale and
851 landscape setting. *Ecological Economics* 35: 25-33.
852 Möller, I., M. Kudella, F. Rupprecht, T. Spencer, M. Paul, B.K. van Wesenbeeck, G. Wolters,
853 K. Jensen, T.J. Bouma, M. Miranda-Lange, and S. Schimmels. 2014. Wave attenuation
854 over coastal salt marshes under storm surge conditions. *Nature Geoscience* 7: 727-731.
855 Möller, I., T. Spencer, J.R. French, D.J. Leggett, and M. Dixon. 1999. Wave transformation
856 over salt marshes: A field and numerical modelling study from north Norfolk, England.
857 *Estuarine Coastal and Shelf Science* 49: 411-426.
858 Mudd, S.M., S.M. Howell, and J.T. Morris. 2009. Impact of dynamic feedbacks between
859 sedimentation, sea-level rise, and biomass production on near-surface marsh
860 stratigraphy and carbon accumulation. *Estuarine Coastal and Shelf Science* 82: 377-
861 389.
862 Murphy, J., and J.P. Riley. 1962. A modified single solution method for the determination of
863 phosphate in natural waters. *Analytica Chimica Acta* 27: 31-36.
864 Najjar, R.G., M. Herrmann, R. Alexander, E.W. Boyer, D.J. Burdige, D. Butman, W.J. Cai,
865 E.A. Canuel, R.F. Chen, M.A.M. Friedrichs, R.A. Feagin, P.C. Griffith, A.L. Hinson,
866 J.R. Holmquist, X. Hu, W.M. Kemp, K.D. Kroeger, A. Mannino, S.L. McCallister,
867 W.R. McGillis, M.R. Mulholland, C.H. Pilskaln, J. Salisbury, S.R. Signorini, P. St-
868 Laurent, H. Tian, M. Tzortziou, P. Vlahos, Z.A. Wang, and R.C. Zimmerman. 2018.
869 Carbon budget of tidal wetlands, estuaries, and shelf waters of eastern North America.
870 *Global Biogeochemical Cycles* 32: 389-416.
871 Niklas, K.J. 2006. A phyletic perspective on the allometry of plant biomass-partitioning
872 patterns and functionally equivalent organ-categories. *New Phytologist* 171: 27-40.
873 Odum, W. 1988. Comparative ecology of tidal freshwater and salt marshes. *Annual Review of*
874 *Ecology and Systematics* 19: 147-176.
875 Ouyang, X.G., and S.Y. Lee. 2020. Improved estimates on global carbon stock and carbon
876 pools in tidal wetlands. *Nature Communications* 11: 317.
877 https://doi.org/10.1038/s41467-019-14120-2.
878 Peck, E.K., R.A. Wheatcroft, and L.S. Brophy. 2020. Controls on sediment accretion and blue
879 carbon burial in tidal saline wetlands: Insights from the Oregon coast, USA. *Journal of*

880 *Geophysical Research-Biogeosciences* 125: e2019JG005464.
881 https://doi.org/10.1029/2019JG005464.
882 Pérez-Harguindeguy, N., S. Díaz, E. Garnier, S. Lavorel, H. Poorter, P. Jaureguiberry, M.S.
883 Bret-Harte, W.K. Cornwell, J.M. Craine, D.E. Gurvich, C. Urcelay, E.J. Veneklaas, P.B.
884 Reich, L. Poorter, I.J. Wright, P. Ray, L. Enrico, J.G. Pausas, A.C. de Vos, N.
885 Buchmann, G. Funes, F. Quétier, J.G. Hodgson, K. Thompson, H.D. Morgan, H. ter
886 Steege, M.G.A. van der Heijden, L. Sack, B. Blonder, P. Poschlod, M.V. Vaieretti, G.
887 Conti, A.C. Staver, S. Aquino, and J.H.C. Cornelissen. 2013. New handbook for
888 standardised measurement of plant functional traits worldwide. *Australian Journal of*
889 *Botany* 61: 167-234.
890 Puijalon, S., T.J. Bouma, C.J. Douady, J. van Groenendael, N.P.R. Anten, E. Martel, and G.
891 Bornette. 2011. Plant resistance to mechanical stress: evidence of an avoidance-
892 tolerance trade-off. *New Phytologist* 191: 1141-1149.
893 R Core Team. 2017. R: A language and environment for statistical computing. *R Foundation*
894 *for Statistical Computing, R Foundation for Statistical Computing, Vienna, Austria*
895 *http://www.R-project.org/*.
896 Rasband, W.S. 1997-2018. ImageJ, 1.53e. Bethesda, Maryland, USA: U.S. National Institutes
897 of Health.
898 Rasse, D.P., C. Rumpel, and M.F. Dignac. 2005. Is soil carbon mostly root carbon?
899 Mechanisms for a specific stabilisation. *Plant and Soil* 269: 341-356.
900 Rayner, D., W. Glamore, L. Grandquist, J. Ruprecht, K. Waddington, and D. Khojasteh. 2021.
901 Intertidal wetland vegetation dynamics under rising sea levels. *Science of the Total*
902 *Environment* 766: 8, 144237. https://doi.org/10.1016/j.scitotenv.2020.144237.
903 Reidenbach, M.A., and E.L. Thomas. 2018. Influence of the seagrass, *Zostera marina*, on
904 wave attenuation and bed shear stress within a shallow coastal bay. *Frontiers in Marine*
905 *Science* 5: 397. https://doi.org/10.3389/fmars.2018.00397.
906 Reise, K. 2005. Coast of change: habitat loss and transformations in the Wadden Sea.
907 *Helgoland Marine Research* 59: 9-21.
908 Riis, T., M. Kelly-Quinn, F.C. Aguiar, P. Manolaki, D. Bruno, M.D. Bejarano, N. Clerici,
909 M.R. Fernandes, J.C. Franco, N. Pettit, A.P. Portela, O. Tammeorg, P. Tammeorg, P.M.
910 Rodriguez-Gonzalez, and S. Dufour. 2020. Global overview of ecosystem services
911 provided by riparian vegetation. *Bioscience* 70: 501-514.

912 Robertson, G.P., and E.A. Paul. 2000. Decomposition and soil organic matter dynamics. In
913 *Methods in Ecosystem Science.*, ed. O.E. Sala, R.B. Jackson, H.A. Mooney and R.W.
914 Howarth, 104-116. New York: Springer.
915 Rothmaler, W. 2007. *Exkursionsflora von Deutschland. Gefäßpflanzen: Atlasband*. München,
916 Germany: Elsevier GmbH.
917 Royston, P. 1982. An extension of Shapiro and Wilk's W test for normality to large samples.
918 *Applied Statistics* 31: 115-124.
919 RStudio Team. 2021. RStudio: Integrated development environment for R. Boston, MA,
920 USA: RStudio, PBC.
921 Rupprecht, F., I. Möller, B. Evans, T. Spencer, and K. Jensen. 2015. Biophysical properties of
922 salt marsh canopies: Quantifying plant stem flexibility and above ground biomass.
923 *Coastal Engineering* 100: 48-57.
924 Sarkar, D. 2008. *Lattice: Multivariate data visualization with R*. New York: Springer.
925 Schepers, L., M. Kirwan, G. Guntenspergen, and S. Temmerman. 2017. Spatio-temporal
926 development of vegetation die-off in a submerging coastal marsh. *Limnology and*
927 *Oceanography* 62: 137-150.
928 Schlichting, E., H.P. Blume, and K. Stahr. 1995. *Bodenkundliches Praktikum*. Berlin:
929 Blackwell.
930 Schmeil, O., and J. Fitschen. 2003. *Flora von Deutschland und angrenzender Länder*.
931 Wiebelsheim, Germany: Quelle & Meier Verlag.
932 Schoutens, K., M. Heuner, E. Fuchs, V. Minden, T. Schulte-Ostermann, J.P. Belliard, T.J.
933 Bouma, and S. Temmerman. 2020. Nature-based shoreline protection by tidal marsh
934 plants depends on trade-offs between avoidance and attenuation of hydrodynamic
935 forces. *Estuarine Coastal and Shelf Science* 236:106645.
936 https://doi.org/10.1016/j.ecss.2020.106645
937 Schoutens, K., M. Heuner, V. Minden, T. Schulte Ostermann, A. Silinski, J.-P. Belliard, and
938 S. Temmerman. 2019. How effective are tidal marshes as nature-based shoreline
939 protection throughout seasons? *Limnology and Oceanography* 64: 1750-1762.
940 Schulte Ostermann, T., M. Heuner, E. Fuchs, S. Temmerman, K. Schoutens, T.J. Bouma, and
941 V. Minden. 2021a. Unraveling plant strategies in tidal marshes by investigating plant
942 traits and environmental conditions. *Journal of Vegetation Science* 32: 1-17.
943 Schulte Ostermann, T., M. Kleyer, M. Heuner, E. Fuchs, S. Temmerman, K. Schoutens, J.T.
944 Bouma, and V. Minden. 2021b. Hydrodynamics affect plant traits in estuarine ecotones

945 with impact on carbon sequestration potentials. *Estuarine Coastal and Shelf Science* 32:
946 e13038. https://doi.org/10.1111/jvs.13038.
947 Scurlock, J.M.O., K. Johnson, and R.J. Olson. 2002. Estimating net primary productivity from
948 grassland biomass dynamics measurements. *Global Change Biology* 8: 736-753.
949 Silinski, A., M. Heuner, J. Schoelynck, S. Puijalon, U. Schroder, E. Fuchs, P. Troch, T.J.
950 Bouma, P. Meire, and S. Temmerman. 2015. Effects of wind waves versus ship waves
951 on tidal marsh plants: A flume study on different life stages of *Scirpus maritimus*. *Plos*
952 *One* 10: e0118687. https://doi.org/10.1371/journal.pone.0118687.
953 Suchrow, S., and K. Jensen. 2010. Plant species responses to an elevational gradient in
954 German North Sea salt marshes. *Wetlands* 30: 735-746.
955 Suding, K.N., S. Lavorel, F.S. Chapin III, J.H.C. Cornelissen, S. Díaz, E. Garnier, D.E.
956 Goldberg, D.U. Hooper, S.T. Jackson, and M.L. Navas. 2008. Scaling environmental
957 change through the community-level: a trait-based response-and-effect framework for
958 plants. *Global Change Biology* 14: 1125-1140.
959 Takahashi, H., T. Yamauchi, T.D. Colmer, and M. Nakazono. 2014. Aerenchyma formation
960 in plants. In *Low-oxygen stress in plants: Oxygen sensing and adaptive responses to*
961 *hypoxia*, ed. J.T. van Dongen and F. Licausi, 247-265. Vienna, Austria: Springer.
962 Temmerman, S., and M.L. Kirwan. 2015. Building land with a rising sea. *Science* 349: 588-
963 589.
964 Temmerman, S., P. Meire, T.J. Bouma, P.M.J. Herman, T. Ysebaert, and H.J. De Vriend.
965 2013. Ecosystem-based coastal defence in the face of global change. *Nature* 504: 79-83.
966 Tremp, H. 2005. *Aufnahme und Analyse vegetationsökologischer Daten*. Stuttgart: Ulmer.
967 UNESCO. 1981. International oceographic tables. *Unesco technical papers in marine science*
968 *39* 3: retreived from (15.05.2023):
969 https://unesdoc.unesco.org/ark:/48223/pf0000047931/PDF/0000047931qaab.pdf.multi.
970 Ungar, I.A. 1991. *Ecophysiology of vascular halophytes*. Boca Raton, Florida CRC Press.
971 van Wesenbeeck, B.K., C.M. Crain, A.H. Altieri, and M.D. Bertness. 2007. Distinct habitat
972 types arise along a continuous hydrodynamic stress gradient due to interplay of
973 competition and facilitation. *Marine Ecology Progress Series* 349: 63-71.
974 Venables, W.N., and B.D. Ripley. 2002. *Modern applied statistics with S*. New York:
975 Springer.
976 Violle, C., M.-L. Navas, D. Vile, E. Kazakou, C. Fortunell, I. Hummel, and E. Garnier. 2007.
977 Let the concept of trait be functional! *Oikos* 116: 882-892.

978 Vousdoukas, M.I., L. Mentaschi, J. Hinkel, P.J. Ward, I. Mongelli, J.C. Ciscar, and L. Feyen.
979 2020. Economic motivation for raising coastal flood defenses in Europe. *Nature*
980 *Communications* 11: 2119. https://doi.org/10.1038/s41467-020-15665-3.
981 Vuik, V., H.Y.S. Heo, Z.C. Zhu, B.W. Borsje, and S.N. Jonkman. 2018. Stem breakage of salt
982 marsh vegetation under wave forcing: A field and model study. *Estuarine Coastal and*
983 *Shelf Science* 200: 41-58.
984 Waltham, N.J., C. Alcott, M.A. Barbeau, J. Cebrian, R.M. Connolly, L.A. Deegan, K. Dodds,
985 L.A.G. Gaines, B. Gilby, C.J. Henderson, C.M. McLuckie, T.J. Minello, G.S. Norris, J.
986 Ollerhead, J. Pahl, J.F. Reinhardt, R.J. Rezek, C.A. Simenstad, J.A.M. Smith, E.L.
987 Sparks, L.W. Staver, S.L. Ziegler, and M.P. Weinstein. 2021. Tidal marsh restoration
988 optimism in a changing climate and urbanizing seascape. *Estuaries and Coasts* 44:
989 1681-1690.
990 Wang, F.M., K.D. Kroeger, M.E. Gonneea, J.W. Pohlman, and J.W. Tang. 2019. Water
991 salinity and inundation control soil carbon decomposition during salt marsh restoration:
992 An incubation experiment. *Ecology and Evolution* 9: 1911-1921.
993 Wang, F.M., C.J. Sanders, I.R. Santos, J.W. Tang, M. Schuerch, M.L. Kirwan, R.E. Kopp, K.
994 Zhu, X.Z. Li, J.C. Yuan, W.Z. Liu, and Z.A. Li. 2021. Global blue carbon accumulation
995 in tidal wetlands increases with climate change. *National Science Review* 8: nwaa296.
996 https://doi.org/10.1093/nsr/nwaa296.
997 Wardle, D.A., K.I. Bonner, and G.M. Barker. 2002. Linkages between plant litter
998 decomposition, litter quality, and vegetation responses to herbivores. *Functional*
999 *Ecology* 16: 585-595.
1000 Warton, D., R.A. Duursma, S. Daniel, and S. Taskinen. 2012. smatr 3 - an R package for
1001 estimation and inference about allometric lines. *Methods in Ecology and Evolution* 3:
1002 257-259.
1003 Warton, D., E.J. Wright, D.S. Falster, and M. Westoby. 2006. Bivariate line-fitting methods
1004 for allometry. *Biological Reviews* 81: 259-291.
1005 Wasserstraßen- und Schifffahrtsdirektion Nord. 2011. *Jahresbericht 2011 Wasser- und*
1006 *Schifffahrtsdirektion Nord*: Kiel: Wasser- und Schifffahrtsdirektion Nord.
1007 Weiher, E., and P.A. Keddy. 1999. Assembly rules as general constraints on community
1008 composition. In *Ecological Assembly Rules: Perspectives, Advances, Retreats*, ed. E.
1009 Weiher and P.A. Keddy, 251-271. Cambridge: Cambridge University Press.

Weiher, E., A. van der Werf, K. Thompson, M. Roderick, E. Garnier, and O. Eriksson. 1999. Challenging Theophrastus: A common core list of plant traits for functional ecology. *Journal of Vegetation Science* 10: 609-620.

White, T.A., D.J. Barker, and K.J. Moore. 2004. Vegetation diversity, growth, quality and decomposition in managed grasslands. *Agriculture Ecosystems & Environment* 101: 73-84.

Wolters, M., A. Garbutt, and J.P. Bakker. 2005. Salt-marsh restoration: evaluating the success of de-embankments in north-west Europe. *Biological Conservation* 123: 249-268.

World Ports Sustainability Program. 2018. Port of Hamburg - Taking Action/Creating Values.

Yan, B.G., Z.H. Ji, B. Fan, X.M. Wang, G.X. He, L.T. Shi, and G.C. Liu. 2016. Plants adapted to nutrient limitation allocate less biomass into stems in an arid-hot grassland. *New Phytologist* 211: 1232-1240.

Zedler, J.B., T. Winfield, and P. Williams. 1980. Salt marsh productivity with natural and altered tidal circulation. *Oecologia* 44: 236-240.

Zhu, Z.C., Z.F. Yang, and T.J. Bouma. 2020. Biomechanical properties of marsh vegetation in space and time: effects of salinity, inundation and seasonality. *Annals of Botany* 125: 277-289.

Figure legends:

Figure 1:

Position of study sites in the Elbe Estuary, north Germany, with 28 plots per study site distributed over four different vegetation zones ranging from the edge of the mudflat to the high bank. The vegetation zones are illustrated for Hollerwettern, with a *Schoenoplectus tabernaemontani*-zone (white circle), a *Bolboschoenus maritimus*-zone (white triangle), a *Phragmites australis*-zone (white square) and a *Phragmites australis*/mixed community-zone (white x). Left: ATKIS® Base-DLM, middle: ©OpenStreetMap contributors, right: © 2016 WSV, BfG, BAW.

Figure 2: Schematic of the species at the study sites, sorted by their occurrence along the elevational gradient, and overview of intensity of the abiotic conditions (inundation duration, soil N_{min}) as well as distribution of trait values (leaf chlorophyll, specific leaf area, stem flexibility and stem specific density). The zone below the mean tidal high water (MHW) level is dominated by *S. tabernaemontani* and *B. maritimus*. The zone above the MHW level is dominated by *P. australis* growing in monotypic stands close to the MHW level and in a mix with species at higher elevations. Species names according to numbers: 1: *Schoenoplectus tabernaemontani* (C.C. Gmel.), 2: *Bolboschoenus maritimus* (L.), 3: *Myosotis scorpioides* (L.), 4: *Typha angustifolia* (L.), 5: *Lythrum salicaria* (L.), 6: *Agrostis stolonifera* (L.), 7: *Lycopus europaeus* (L.), 8: *Phragmites australis* (Cav.), 9: *Phalaris arundinacea* (L.), 10: *Mentha aquatica* (L.)/*Mentha verticillata* (L.), 11: *Juncus gerardii* (Loisel.), 12: *Cirsium arvense* (L.) 13: *Festuca arundinacea* (Scop.), 14: *Elymus athericus* (Link), 15: *Calystegia sepium* (L.), 16: *Scutellaria galericulata* (L.)

Figure 3: Environmental variables for the tidal marsh zone below the mean high water level (below the MHW level, light grey bars) and above the MHW level (dark grey bars) with standard deviations. Significant differences are indicated with * $p<0.05$, ** $p<0.01$ and ***$p<0.001$, tested with a t-test. Nonsignificant differences are indicated with NS.

Figure 4: Ecosystem properties (upper row) and ecosystem services (lower row) for the tidal marsh zone below the mean high water level (below the MHW level, light grey bars) and above the MHW level (dark grey bars) with standard deviations. Significant differences are indicated with * $p<0.05$, ** $p<0.01$ and ***$p<0.001$, tested with a t-test. Nonsignificant differences are indicated with NS.

Figure 5: Results of multiple linear regression (MLR). All graphs refer to the tidal zone below the MHW level. Wire graphs include a) wave attenuation [m], AGB (aboveground community biomass [g m^{-2}]) and trait aggregate 'stem traits' (SSD, SDMC, fresh mass per volume, and Young's modulus), b) AGB (aboveground community biomass [g/m^2]), trait aggregate 'stem traits' (SSD, SDMC, fresh mass per volume and Young's modulus) and trait aggregate 'leaf traits' (total leaf area and LDMC), c) SOC (soil organic carbon [%]), inundation duration (square root transformed), and trait aggregate 'stem traits' (SSD, SDMC, fresh mass per volume and Young's modulus).

Figure 6: Results of multiple linear regression (MLR). All graphs refer to the tidal zone above the MHW level. Wire graphs include a) decomposition rate [%/day], inundation [hr/day, square root transformed] and trait aggregate 'stem traits' (SSD, SDMC, fresh mass per volume and Young's modulus) and b) SOC density (soil organic carbon density [kg/m^3]), decomposition rate [%/day] and trait aggregate 'stem traits' (SSD, SDMC, fresh mass per volume and Young's modulus).

Table 1: Environmental variables, plant traits and ecosystem properties with abbreviations, transformations used and units. For the plant traits, the aggregates are indicated. For details on the aggregates, see Table 2.

Environmental variable		**Abbreviation**	**Transformation**	**Unit**
Inundation			Square root	hr/day
Soil salinity				PSU
Soil carbonate				kg/m^2
Clay content		$CaCO_3$		kg/m^2
Sand content				kg/m^2
Plant available nitrogen		N_{min}		g/m^2
Soil phosphorus content		Soil P		g/m^2
Soil potassium content		Soil K		g/m^2
Plant traits	**Aggregate**	**Abbreviation**	**Transformation**	**Unit**
Canopy height				cm
Stem mass to volume	**Stem traits**			$g_{fresh\ mass}/cm^3$
Young's modulus			log	MPa
Stem specific density		SSD	Tukey	$g_{dry\ mass}/cm^3$
Stem dry matter content		SDMC	log	$mg_{dry\ mass}/g_{fresh\ mass}$
Leaf dry matter content	**Leaf traits**	LDMC	Tukey	$mg_{dry\ mass}/g_{fresh\ mass}$
Total leaf area			log	mm^2
Stem mass	**Mass**		log	g
Leaf mass			log	g
Root mass			log	g
Rhizome mass			log	g
Root dry matter content	**Belowground traits**	RDMC		$mg_{dry\ mass}/g_{fresh\ mass}$
Rhizome dry matter content		RHDMC		$mg_{dry\ mass}/g_{fresh\ mass}$
Root specific density		RSD	square root	$g_{dry\ mass}/cm^3$
Rhizome specific density		RHSD	log	$g_{dry\ mass}/cm^3$
Root specific length		RSL	log	$mm/g_{dry\ mass}$
Rhizome specific length		RHSL	log	$mm/g_{dry\ mass}$
N:P ratio leaf	**Leaf stoichiometry**	N:P leaf		
C:N ratio leaf		C:N leaf	Tukey	
Ecosystem properties		**Abbreviation**	**Transformation**	**Unit**
Aboveground biomass		AGB		g/m^2
Vegetation density		PAR		%
Decomposition native litter		Decomp. native		% /day
Decomposition standard hay		Decomp. standard		% /day
Ecosystem services				
Wave attenuation				m/m
Soil organic carbon content		SOC.content	log	%
Soil organic carbon density		SOC.density		kg/m^3

Table 2: Aggregated trait variables and the variances explained by the first two PCA axes for each of the tidal zones below the MHW level and above the MHW level. All PCAs were significant at $p<0.05$. For the traits constituting each aggregate, see Table 1.

Aggregated trait variables	PCA axis 1 – below MHW	PCA axis 2 – below MHW	PCA axis 1 – above MHW	PCA axis 2 – above MHW
Stem traits	0.91	0.07	0.72	0.16
Leaf traits	0.77	0.23	0.81	0.19
Mass	0.66	0.27	0.77	0.17
Belowground traits	0.53	0.32	0.61	0.24
Leaf stoichiometry	0.96	0.03	0.82	0.18

The aggregate 'stem traits' include stem mass per volume, Young's modulus, stem specific density and stem dry matter content. The aggregate 'leaf traits' include leaf dry matter content and total leaf area. The aggregate 'mass' comprises the total biomass of stems, leaves, roots and rhizomes, and the aggregate 'belowground traits' are root dry matter content, rhizome dry matter content, root specific density, rhizome specific density, root specific length and rhizome specific length (the last two with inverted values).

Table 3: Standard major axis regression (SMA) for trait aggregates above and below the mean high water (MHW) level with correlation coefficients, R^2 and associated intercepts (α) and slopes (β). * p<0.05, ** p<0.01 and ***p<0.001

Aggregate A	Aggregate B		Correl.	R^2	α	β		Correl.	R^2	α	β
leaf traits	stem traits	Below mean high water level	0.81	0.66 ***	$-6.9e^{-16}$	0.65	Above mean high water level	0.76	0.58 ***	$6.4e^{-16}$	0.75
stem traits	mass		-0.05	0.002	-	-		0.59	0.36 ***	$-1.7e^{-15}$	0.96
belowgr. traits	stem traits		-0.10	0.01	-	-		0.89	0.80 ***	$1.9e^{-15}$	1.13
leaf stoich.	stem traits		0.81	0.67 ***	$-1.7e^{-15}$	0.73		0.52	0.28 ***	$5.8e^{-17}$	0.76
leaf traits	mass		-0.43	0.19 **	$-5.5e^{-16}$	-0.76		0.92	0.74 ***	$-6.1e^{-16}$	0.72
leaf traits	belowgr. traits		-0.38	0.14 **	$-8.3e^{-16}$	-0.69		0.82	0.68 ***	$-0.7e^{-16}$	0.66
leaf traits	leaf stoich.		0.96	0.91 ***	$-2.2e^{-15}$	0.89		0.91	0.83 ***	$5.9e^{-16}$	0.99
mass	belowgr. traits		0.04	0.001 **	$3.7e^{-16}$	0.91		0.75	0.56 ***	$-8.3e^{-16}$	0.92
mass	leaf stoich.		-0.36	0.12 *	$2.2e^{-15}$	-1.17		0.85	0.73 ***	$1.7e^{-15}$	1.37
belowgr. traits	leaf stoich.		-0.54	0.29 ***	$2.0e^{-15}$	-1.29		0.71	0.50 ***	$1.9e^{-15}$	1.50
canopy (log)	stem traits		0.66	0.44 ***	4.93	0.14		-0.65	0.42 ***	5.20	-0.15

Table 4: Results of the multiple linear regression model including wave attenuation, AGB, SOC content, aggregate stem traits and leaf traits and the environmental variable inundation for the tidal zone below the MHW level. The estimates, standard error, t-values, and significance levels are given (* p<0.05, ** p<0.01 and ***p<0.001). Measures of model performance are shown below each model.

	Estimate	SE	t
Model a)			
Intercept wave attenuation	0.016	0.002	7.41 ***
AGB^2	<0.001	<0.001	4.78 ***
'stem traits'	0.002	0.001	2.11 *
Adj. R^2 = 0.60; variance explained: 63%; F(3,38) = 21.67, p < 0.001			

	Estimate	SE	t
Model b)			
Intercept AGB	1003.77	43.83	22.90***
'stem traits'	96.19	39.57	2.43*
'leaf traits'	194.88	60.78	3.21 **
Adj. R^2 = 0.67; variance explained: 68%; F(2,39) = 41.77, p < 0.001			

	Estimate	SE	t
Model c)			
Intercept SOC content	1.78	0.67	2.65 *
inundation	-0.53	0.18	-2.98 **
'stem traits'^2	-0.053	0.02	-2.04 *
Adj. R^2 = 0.15; variance explained: 22%; $F(3,38) = 3.50$, $p = 0.02$			

Table 5: Results of the multiple linear regression model including decomposition rates, soil organic carbon density, aggregate stem traits and inundation duration for the tidal zone above the MHW level. The estimates, standard errors, t-values, and significance levels are given (* p<0.05, ** p<0.01 and ***p<0.001). Measures of model performance are shown as well.

	Estimate	SE	t
Model a)			
Intercept Decomp. native^2	0.19	0.007	25.57 ***
Inundation	-0.005	0.001	-3.59 ***
'stem traits'^2	-0.003	0.002	-2.11 **
Adj. R^2 = 0.32; variance explained: 36%; $F(2,39) = 10.85$, $p < 0.001$			

	Estimate	SE	t
Model b)			
Intercept SOC density	1.46	0.31	4.66 ***
Decomp. native	0.09	0.04	2.37 *
'stem traits'^2	0.06	0.02	2.66 *
Adj. R^2 = 0.13; variance explained: 19%; $F(3,38) = 0.04$, $p < 0.05$			

Figure 1

Click here to access/download;Figure;ESCO_Fig.1.tiff

Figure 2

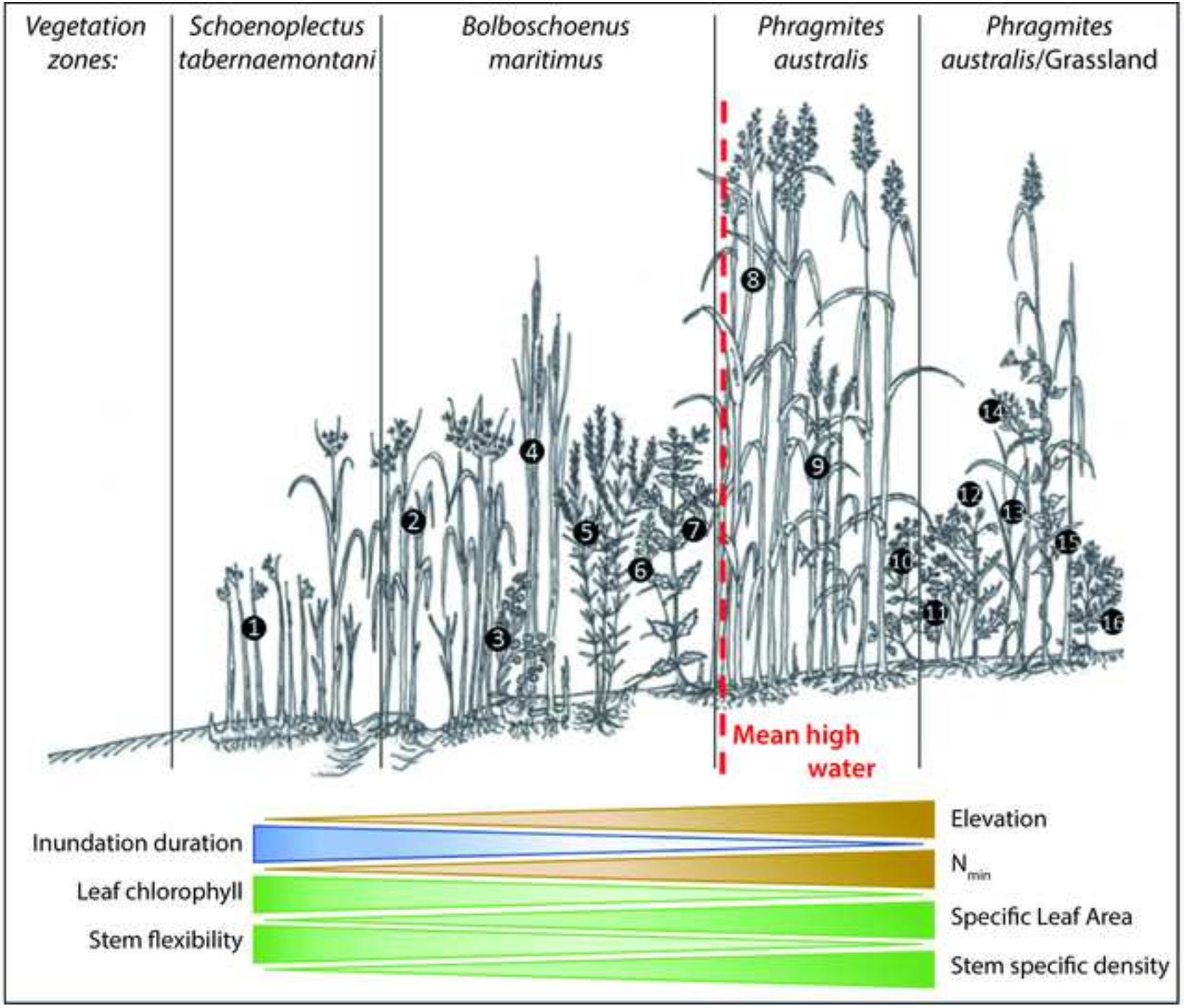

Figure 3

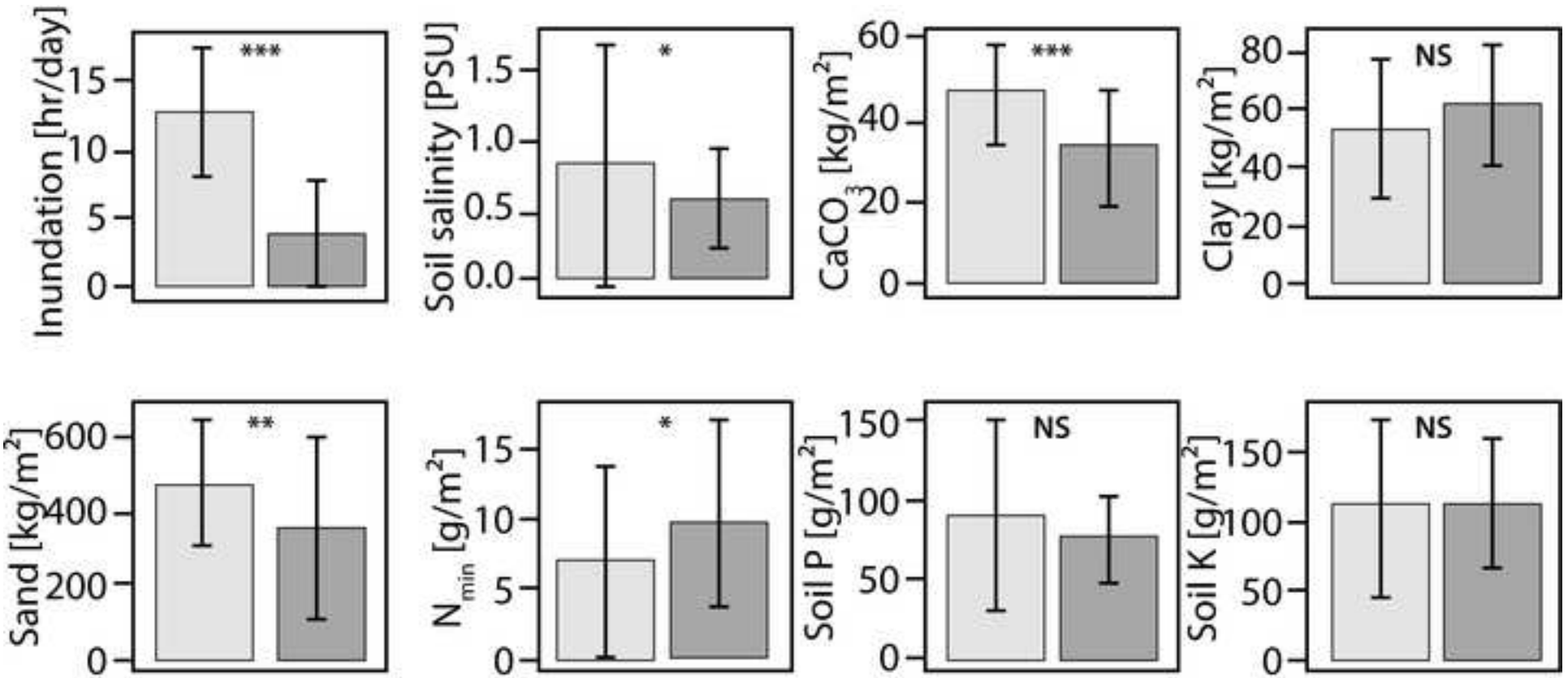

Figure 4

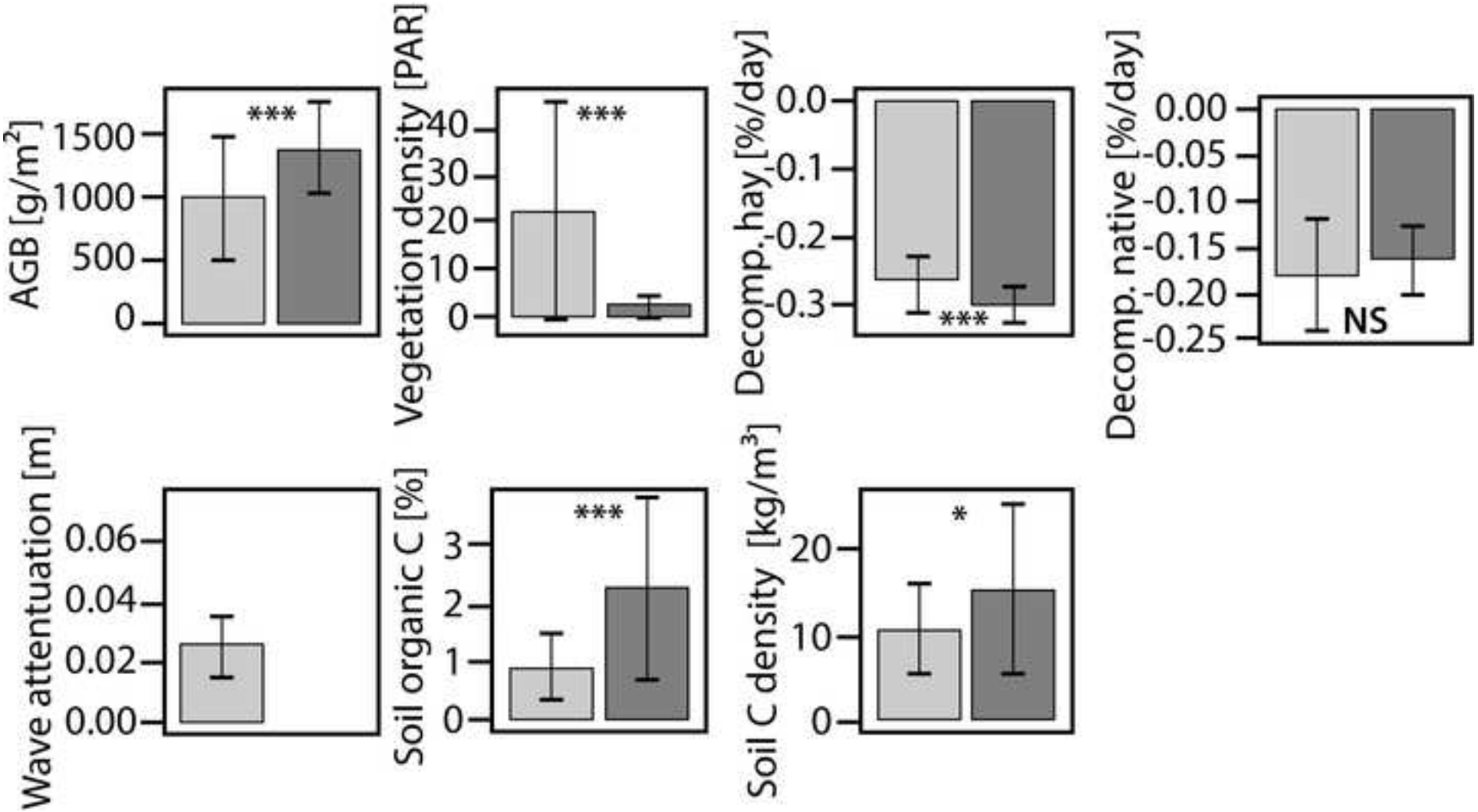

Figure 5

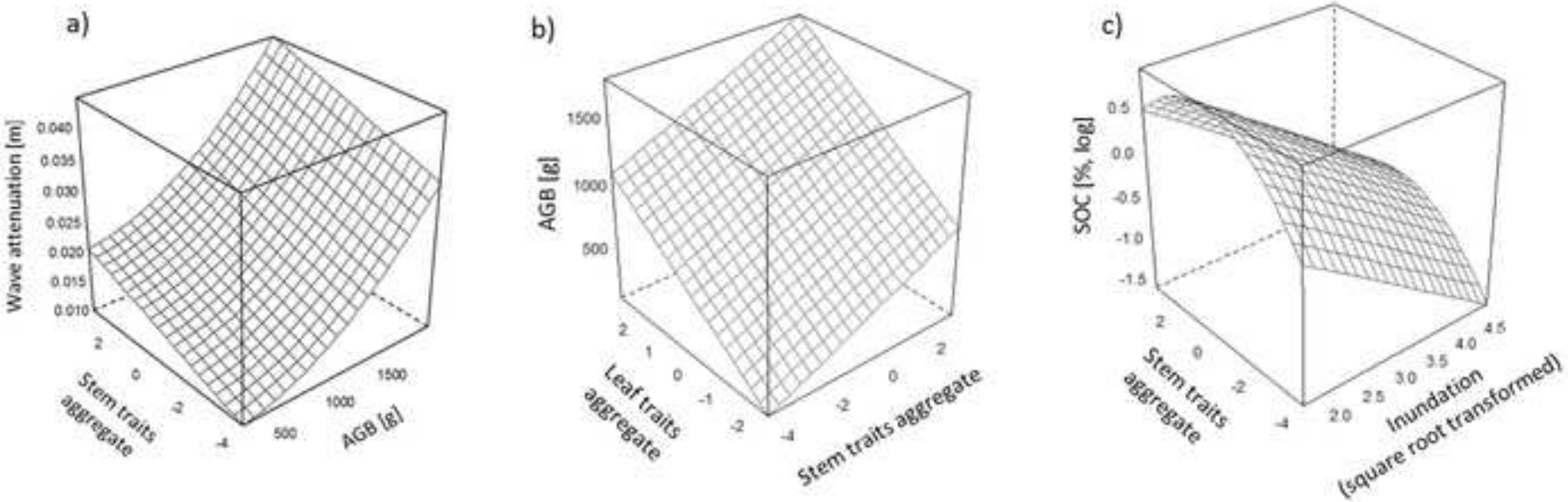

Figure 6

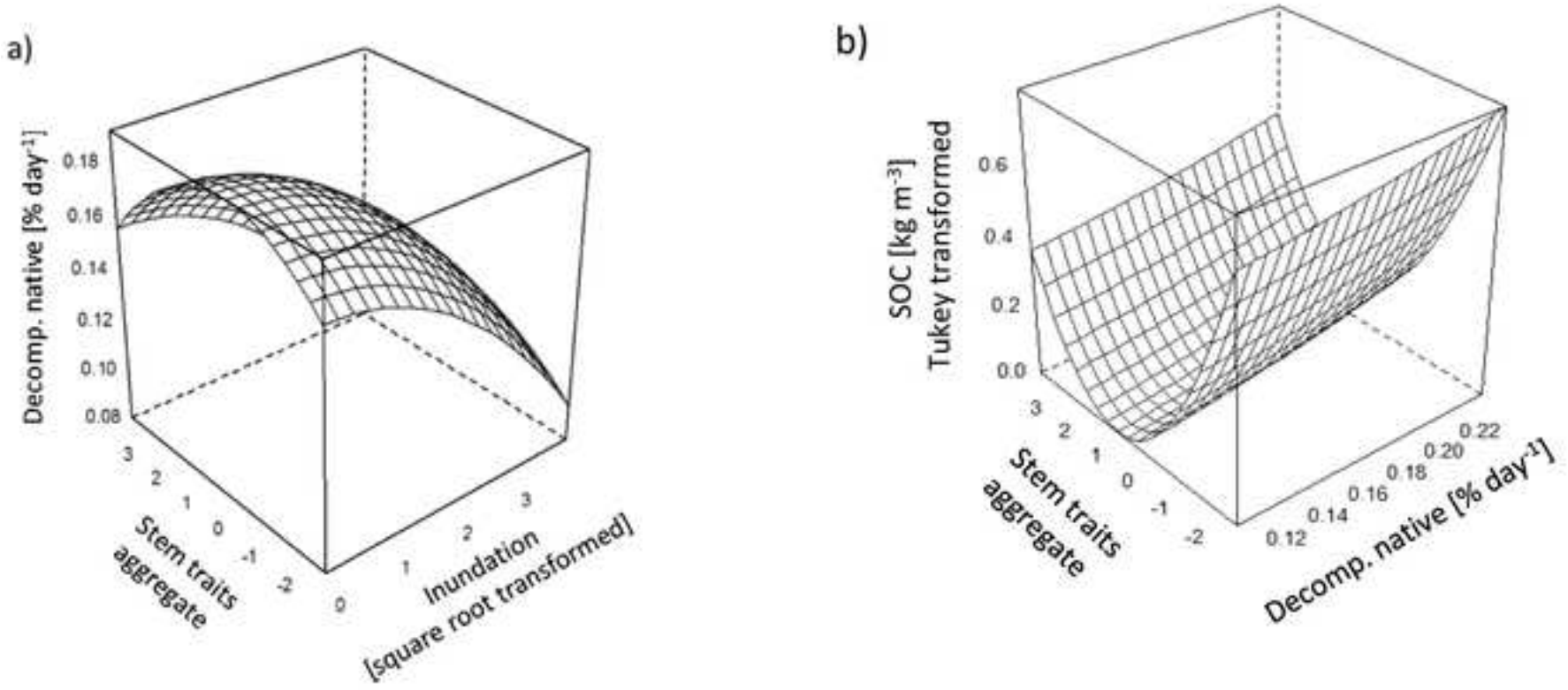

Electronic Supplemental Material: Online Resource 1 24. May 2022

Identifying key plant traits and ecosystem properties affecting wave attenuation and carbon sequestration potential of tidal marshes

Schulte Ostermann, Tilla[1]; Heuner, Maike[2]; Fuchs, Elmar[2]; Temmerman, Stijn[3]; Schoutens, Ken[3]; Bouma, Tjeerd J.[4]; Minden, Vanessa[5]

[1]Landscape Ecology Group, University of Oldenburg, Oldenburg, Germany
[2]Federal Institute of Hydrology, Koblenz, Germany
[3]Ecosphere research group, Department of Biology, University of Antwerp, Wilrijk, Belgium
[4]Royal Netherlands Institute of Sea Research, Yerseke, The Netherlands
[5]Department of Biology, Ecology and Biodiversity, Vrije Universiteit Brussel, Brussels, Belgium

Corresponding author: Vanessa Minden, Department of Biology, Ecology and Biodiversity, Vrije Universiteit Brussel, Brussels, Belgium. +32 2 629 3423, email: vanessa.minden@vub.be

Keywords: ecosystem properties, ecosystem services, estuarine vegetation, plant traits, soil organic carbon

Appendix S1: Equations used for the calculation of Young´s modulus.

The equation needed for the calculation of Young´s modulus is: $= \frac{EI}{I}$. The elements needed are Flexural stiffness (*EI*), which can be calculated for all stem shapes as: $EI = \frac{s^3}{48} * \frac{F}{D}$. s is the support distance set on the Instron (at least 15x stem diameter, see Usherwood et al. 1997) and $\frac{F}{D}$ is the force/deflection slope, derived from the bending tests.

Further, the second moment of area (I) for round hollow stems (such as *Phagmites australis*) is calculated as $I = \frac{\pi}{4} * (r_{out}^4 - r_{inn}^4)$ where r = radius, out = outer and inn = inner. For round filled stems (like *Schoenoplectus tabernaemontani*) it is calculated through $I = \pi * \frac{d^4}{64}$, with d being the diameter. For triangular stems (like *Bolboschoenus maritimus)* the calculation is: $I = \frac{\sqrt{3}}{96} * bv^4$ where bv is the basal length of the triangle. For square stems (such as *Mentha aquatica*) the equation for the second moment of area is: $I = b * \frac{b^3}{12}$, with b being the side length.

Appendix S2: Calculation of wave attenuation for the zone below the mean high tide level.

For the estimation of wave height reduction (attenuation), the mean wave height was used for water depth <0.5m for all measurement points in the first two vegetation zones below mean high tide and dominated by *Schoenoplectus tabernaemontani* and *Bolboschoenus maritimus*. Test for significant regressions were performed for the different sites. The attenuation is the difference in incoming wave height and height after a certain distance and at a higher elevation. We used the following regression equation for wave attenuation ($Atten_{Hmean}$) and adjustment for plot elevation (znorm_diff):

$Atten_{Hmean}$ = 0.093670 * znorm_diff + 0.010679

For further description of the method, see Schoutens et al. (2019) and Schoutens et al. (2020)

Schoutens, K., M. Heuner, E. Fuchs, V. Minden, T. Schulte-Ostermann, J.P. Belliard, T.J. Bouma, and S. Temmerman. 2020. Nature-based shoreline protection by tidal marsh plants depends on trade-offs between avoidance and attenuation of hydrodynamic forces. *Estuarine Coastal and Shelf Science* 236: 11.

Schoutens, K., M. Heuner, V. Minden, T. Schulte Ostermann, A. Silinski, J.-P. Belliard, and S. Temmerman. 2019. How effective are tidal marshes as nature-based shoreline protection throughout seasons? *Limnology and Oceanography* 64: 1750-1762.

Usherwood, J.R., A.R. Ennos, and D.J. Ball. 1997. Mechanical and anatomical adaptations in terrestrial and aquatic buttercups to their respective environments. *Journal of Experimental Botany* 48: 1469-1475.

Tidal zone below MWH

Tidal zone above MWH

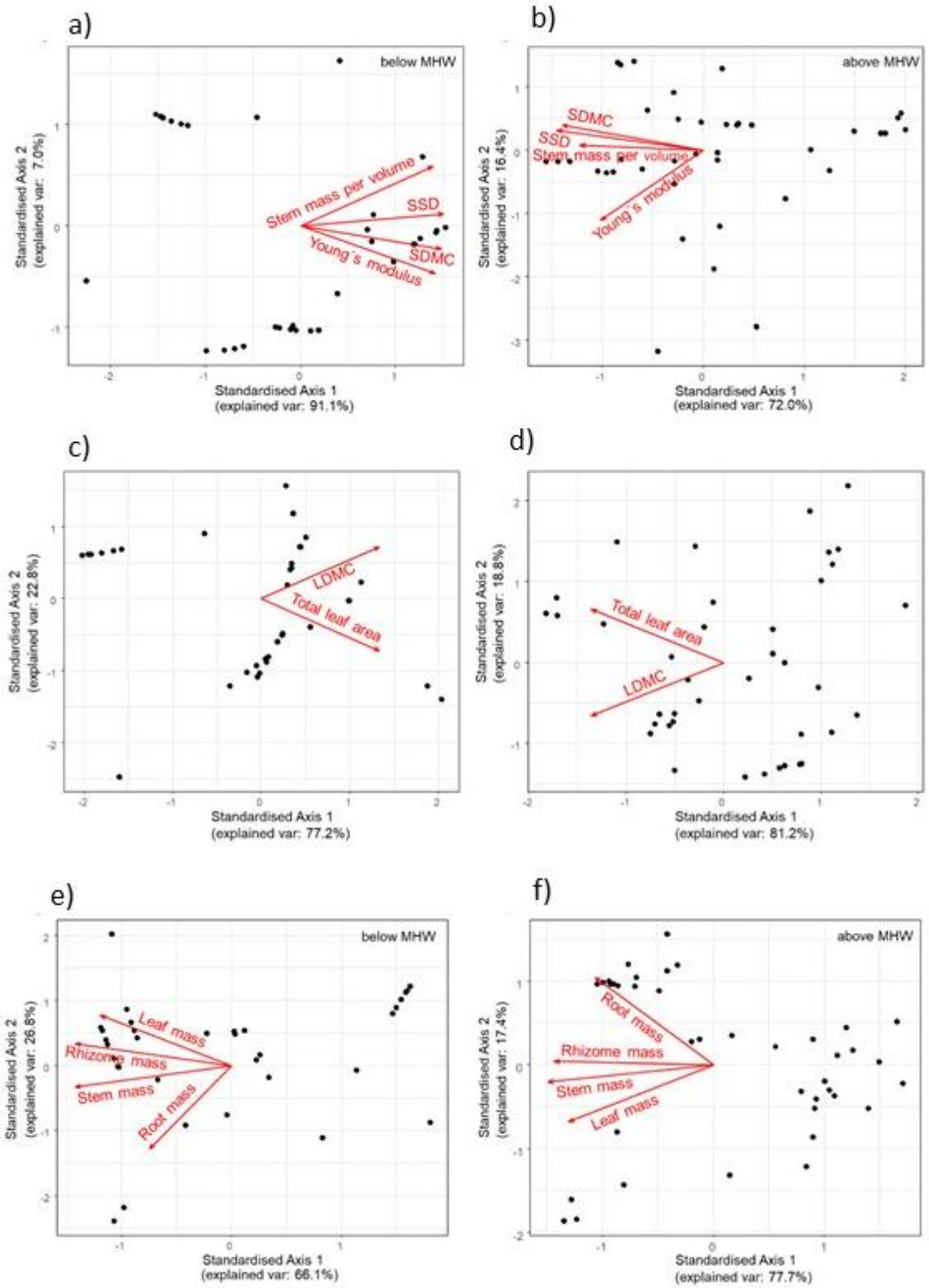

Fig. S1 continued

Tidal zone below MWH Tidal zone above MWH

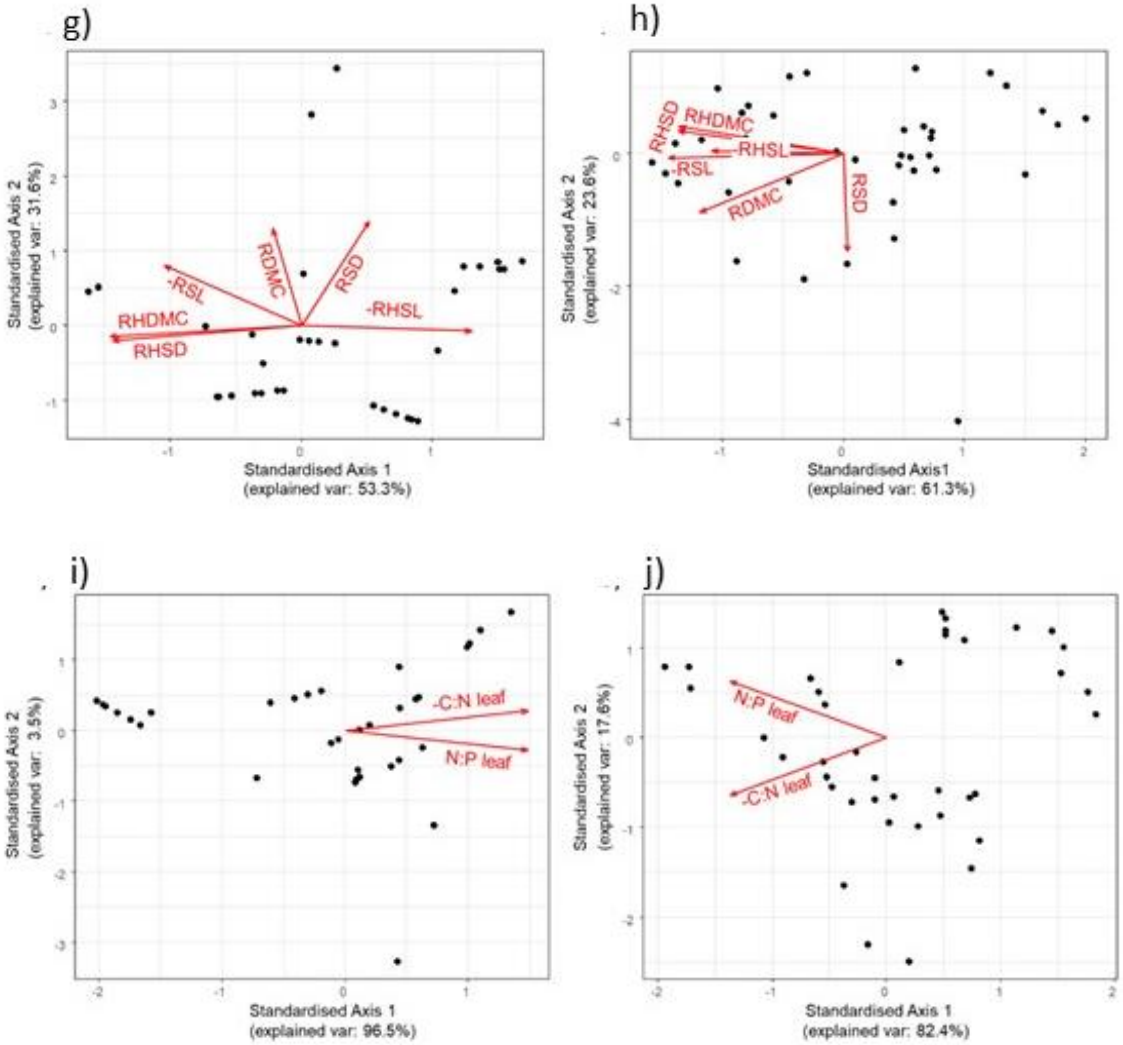

Fig. S1: Graphical output of Principal Component Analysis (PCA) with information on total variance (V_{total}) explained (variance explained by single axes given in the specific graphs) in the tidal zones below and above mean high water level (MHW), respectively. PCAs for the aggregate a) 'stem traits' in the zone below MHW (V_{Total}: 98.1%), b) 'stem traits' in the zone above MHW (V_{Total}: 88.4%), c) 'leaf traits' in the zone below MHW (V_{Total}: 100%), d) 'leaf traits' in the zone above MHW (V_{Total}: 100%), e) 'mass' in the zone below MHW (V_{Total}: 92.9%), f) 'mass' in the zone above MHW (V_{Total}: 95.1%), g) 'belowground traits' in the zone below MHW (V_{Total}: 84.8%), h) 'belowground traits' in the zone above MHW (V_{Total}: 84.9%), i) 'leaf stoichiometry' in the zone below MHW (V_{Total}: 100%), j) 'leaf stoichiometry ' in the zone above MHW (V_{Total}: 100%).

Points represent community weighted means per plot. Variables displayed: Stem mass per volume (stem $g_{fresh\ mass}/cm^3$), stem specific density (SSD, $g_{fresh\ mass}/cm^3$), stem dry matter content (SDMC, $mg_{dry\ mass}/g_{fresh\ mass}$), Young´s modulus = stem resistance to bending (MPa), leaf dry matter content (LDMC, $mg_{dry\ mass}/g_{fresh\ mass}$) and total leaf area ($mm^2$), dry mass for leaves (g), rhizomes (g), stems and roots (g), rhizome specific density (RHSD, $g_{fresh\ mass}/cm^3$), rhizome dry matter content (RHDMC, $mg_{dry\ mass}/g_{fresh\ mass}$), root specific length (RSL, $mm/g_{dry\ mass}$), root dry matter content (RDMC, $mg_{dry\ mass}/g_{fresh\ mass}$), root specific density (RSD, $g_{fresh\ mass}/cm$), rhizome specific length (RHSL, $mm/g_{dry\ mass}$), C:N leaf = carbon/nitrogen ratio of leaf biomass, N:P leaf = nitrogen/phosphorus ratio of leaf biomass.

Table S1: Correlation coefficients of the separate trait-aggregates with the first two corresponding PCA axes.

	Tidal zone below MHW		Tidal zone above MHW	
	PCA1	PCA2	PCA1	PCA2
Aggregate 'stem traits'				
Stem mass per volume	0.47	0.74	-0.48	0.07
Young's modulus	0.49	-0.59	-0.39	-0.91
SSD	0.52	0.15	-0.56	0.26
SDMC	0.51	-0.28	-0.54	0.33
Aggregate 'leaf traits'				
LDMC	0.71	0.71	-0.71	-0.71
Total leaf area	0.71	-0.71	-0.71	0.71
Aggregate 'Mass'				
Stem mass	-0.58	-0.21	-0.56	-0.16
Leaf mass	-0.49	0.49	-0.49	-0.54
Root mass	-0.30	-0.30	-0.40	0.83
Rhizome mass	-0.54	-0.58	-0.54	0.04
Aggregate 'Belowground traits'				
RDMC	-0.08	0.62	-0.41	-0.49
RHDMC	-0.54	-0.07	-0.47	0.23
RSD	0.19	0.67	0.01	-0.82
RHSD	-0.53	-0.09	-0.47	0.19
RSL	-0.38	0.38	-0.49	-0.03
RHSL	0.48	-0.03	-0.38	0.03
Aggregate 'Leaf stoichiometry'				
N:P leaf	0.71	-0.71	-0.71	0.71
C:N leaf	0.71	0.71	-0.71	-0.71

Aggregate 'stem traits': Stem mass per volume (stem $g_{fresh\ mass}/cm^3$), stem resistance to bending (Young´s modulus, MPa), stem specific density (SSD, $g_{fresh\ mass}/cm^3$) and stem dry matter content (SDMC, $mg_{dry\ mass}/g_{fresh\ mass}$). Aggregate 'leaf traits': leaf dry matter content (LDMC, $mg_{dry\ mass}/g_{fresh\ mass}$) and total leaf area ($mm^2$). Aggregate 'Mass': dry mass of stems, leaves, roots and rhizomes (all in g). Aggregate 'Belowground traits': root dry matter content (RDMC, $mg_{dry\ mass}/g_{fresh\ mass}$), rhizome dry matter content (RHDMC, $mg_{dry\ mass}/g_{fresh\ mass}$), root specific density (RSD, $g_{fresh\ mass}/cm^3$), rhizome specific density (RHSD, $g_{fresh\ mass}/cm^3$), root specific length (RSL, $mm/g_{dry\ mass}$) and rhizome specific length (RHSL, $mm/g_{dry\ mass}$). Aggregate 'Leaf stoichiometry': nitrogen/phosphorus ratio of leaf biomass (N:P leaf) and carbon/nitrogen ratio of leaf biomass (C:N leaf).

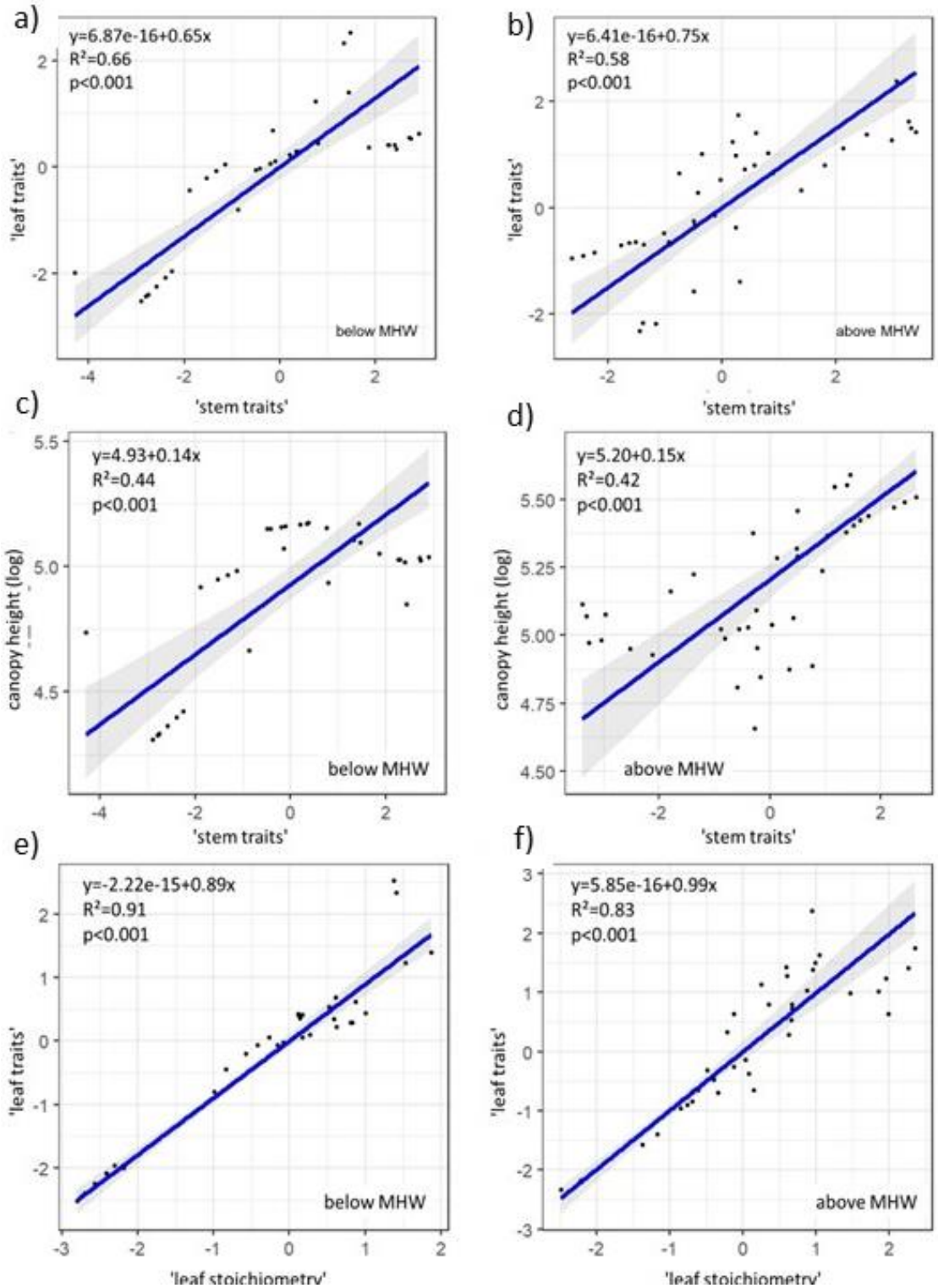

Fig. S2: SMA (standard major axis regression) of different aggregates with 95 % confidence intervals and equations for linear regression lines and R^2 values in the tidal zones below and above mean high water level (MHW), respectively. *For variables combined in trait aggregates and units of variables, see Table 1.* SMA for aggregates a) 'leaf traits' versus 'stem traits' in the zone below MHW, b) 'leaf traits' versus 'stem traits' in the zone above MHW, c) canopy height versus the aggregate 'stem traits' in the zone below MHW, d) for canopy height versus the aggregate 'stem traits' in the zone above MHW, e) 'leaf traits' versus 'leaf stoichiometry' in the zone below MHW, f) 'leaf traits' versus 'leaf stoichiometry' in the zone above MHW.